NUMERICAL MODELS OF SALT MARSH EVOLUTION: ECOLOGICAL, GEOMORPHIC, AND CLIMATIC FACTORS

Sergio Fagherazzi,[1] Matthew L. Kirwan,[2,3] Simon M. Mudd,[4] Glenn R. Guntenspergen,[2] Stijn Temmerman,[5] Andrea D'Alpaos,[6] Johan van de Koppel,[7] John M. Rybczyk,[8] Enrique Reyes,[9] Chris Craft,[10] and Jonathan Clough[11]

Received 25 February 2011; revised 25 June 2011; accepted 8 September 2011; published 6 January 2012.

[1] Salt marshes are delicate landforms at the boundary between the sea and land. These ecosystems support a diverse biota that modifies the erosive characteristics of the substrate and mediates sediment transport processes. Here we present a broad overview of recent numerical models that quantify the formation and evolution of salt marshes under different physical and ecological drivers. In particular, we focus on the coupling between geomorphological and ecological processes and on how these feedbacks are included in predictive models of landform evolution. We describe in detail models that simulate fluxes of water, organic matter, and sediments in salt marshes. The interplay between biological and morphological processes often produces a distinct scarp between salt marshes and tidal flats. Numerical models can capture the dynamics of this boundary and the progradation or regression of the marsh in time. Tidal channels are also key features of the marsh landscape, flooding and draining the marsh platform and providing a source of sediments and nutrients to the marsh ecosystem. In recent years, several numerical models have been developed to describe the morphogenesis and long-term dynamics of salt marsh channels. Finally, salt marshes are highly sensitive to the effects of long-term climatic change. We therefore discuss in detail how numerical models have been used to determine salt marsh survival under different scenarios of sea level rise.

Citation: Fagherazzi, S., et al. (2012), Numerical models of salt marsh evolution: Ecological, geomorphic, and climatic factors, *Rev. Geophys.*, *50*, RG1002, doi:10.1029/2011RG000359.

1. INTRODUCTION

[2] Salt marshes are complex environments located between the sea and land. They are regularly flooded by tides and storm surges and covered by salt-tolerant vegetation, mostly herbs and grasses, that is critical for their stability and trapping of sediments (Figure 1).

[3] Salt marshes occur on low-energy coasts in temperate and high latitudes, both in microtidal and macrotidal regimes [*Allen and Pye*, 1992]. They typically form in sheltered environments where fine sediments can accumulate, such as in estuaries, shallow bays, and on the landward side of barrier islands and spits. Salt marshes are also common near large rivers and deltas, which provide the sediment input necessary for their formation and evolution. Salt marshes are ecologically important components of the coastal landscape because they provide many critical ecosystem functions, such as production of organic material and nutrient cycling [*Weinstein and Kreeger*, 2000]. Because flooding is the main mechanism for sediment delivery to the marsh platform, salt marshes are inextricably linked to sea level and tidal oscillations.

[4] Salt marshes are the manifestation of complex ecological and physical interactions and therefore require an interdisciplinary approach to discern the mechanisms by which they function [*Fagherazzi et al.*, 2004a; *Kirwan and Murray*,

[1]Department of Earth Sciences and Marine Program, Boston University, Boston, Massachusetts, USA.
[2]Patuxent Wildlife Research Center, U.S. Geological Survey, Laurel, Maryland, USA.
[3]Now at Department of Environmental Sciences, University of Virginia, Charlottesville, Virginia, USA.
[4]School of GeoSciences, University of Edinburgh, Edinburgh, UK.
[5]Department of Biology, University of Antwerpen, Antwerp, Belgium.
[6]Department of Geosciences, University of Padova, Padua, Italy.
[7]Spatial Ecology Department, Netherlands Institute of Ecology, Yerseke, Netherlands.
[8]Department of Environmental Sciences, Huxley College of the Environment, Western Washington University, Bellingham, Washington, USA.
[9]Department of Biology, East Carolina University, Greenville, North Carolina, USA.
[10]School of Public and Environmental Affairs, Indiana University, Bloomington, Indiana, USA.
[11]Warren Pinnacle Consulting, Warren, Vermont, USA.

8755-1209/12/2011RG000359
Paper number 2011RG000359

Figure 1. Marsh boundary in Plum Island Sound, Massachusetts, United States, a macrotidal environment dominated by *Spartina* spp. at (a) low and (b) high tides. (c) Network of tidal channels dissecting a salt marsh in the Venice Lagoon, Italy (IKONOS image).

2007; *Marani et al.*, 2007; *Townend et al.*, 2010]. Numerical modeling is one powerful tool that can be used to quantify the nonlinear feedbacks between salt marsh ecosystems, morphology, and sediment transport processes [*Costanza and Voinov*, 2004; *Mcleod et al.*, 2010]. Numerical models can be used to test hypotheses regarding salt marsh processes, quantify the exchanges of energy and material across the intertidal landscape, and shed light on the long-term evolution and resilience of these systems.

[5] Salt marsh models differ in the spatial scales that are considered, the processes that are simulated within the models, and ultimately, the output that is generated by the simulations [*Rybczyk and Callaway*, 2009]. At the smallest scale are the zero-dimensional models that simulate processes (i.e., net primary production and elevation change) at a single point within a marsh. Next are the models that simulate morphodynamics (i.e., sedimentation, channel development, and erosion) across a marsh platform (a two-dimensional model) or a marsh transect (a one-dimensional model). These models are said to be "ecogeomorphic" if they additionally consider the feedbacks between marsh vegetation and physical processes such as sedimentation and erosion. Finally, at the largest scale are the landscape models that simulate processes over entire coastlines or estuaries. In general, landscape models excel at simulating general trends at large spatial scales while the smaller-scale models often provide more mechanistic algorithms to simulate wetland processes.

[6] Salt marsh models usually simulate long time scales, from years to centuries, and therefore particular attention must be devoted to integration errors, which accumulate in the results and predictions. To this end, empirical frameworks based on data collected at the temporal scale of interest are often more suitable, whereas mechanistic models based on a detailed description of the short-term physics might lead to long-term errors.

[7] Here we present a synthesis of several approaches to salt marsh modeling. All models follow a general conceptual framework for salt marsh evolution (Figure 2) [*Fagherazzi et al.*, 2004a; *Ogden et al.*, 2005, *Sklar et al.*, 1990]. First we review physical processes; modeling sediment fluxes across the marsh platform and modeling marsh boundary and channel evolution. Next, because the presence or absence of halophytic vegetation on the marsh surface is fundamental to salt marsh evolution [*Fagherazzi et al.*, 2004b], we review the simulation of aboveground and belowground production. We then shift to larger-scale simulations and review models that simulate coastal marsh evolution at the landscape scale. Finally, because much of the recent salt marsh modeling work has been in response to concerns regarding the effects of rising sea levels on salt marsh evolution and resilience [*Kirwan et al.*, 2010], we review how numerical models have been used to determine the fate of salt marshes under different scenarios of sea level rise.

2. MODELING SEDIMENT FLUXES ON THE MARSH PLATFORM

[8] During flooding, suspended sediments are transported with the tidal currents onto the marsh platform and partially deposited in distinctive spatial patterns. The modeling of these sediment fluxes is particularly relevant from a geomorphic and ecological point of view. The spatial sedimentation patterns that occur during single inundations drive the longer-term geomorphic development of the marsh platform, such as the development of natural levees [e.g., *Temmerman et al.*, 2004]. Also, ecological processes are directly affected

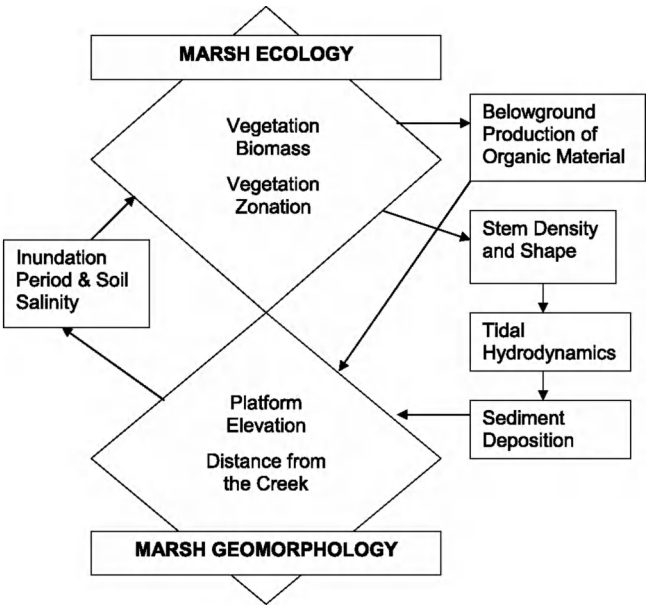

Figure 2. Simplified scheme of the interactions between ecology and geomorphology in salt marshes [after *Fagherazzi et al.*, 2004a].

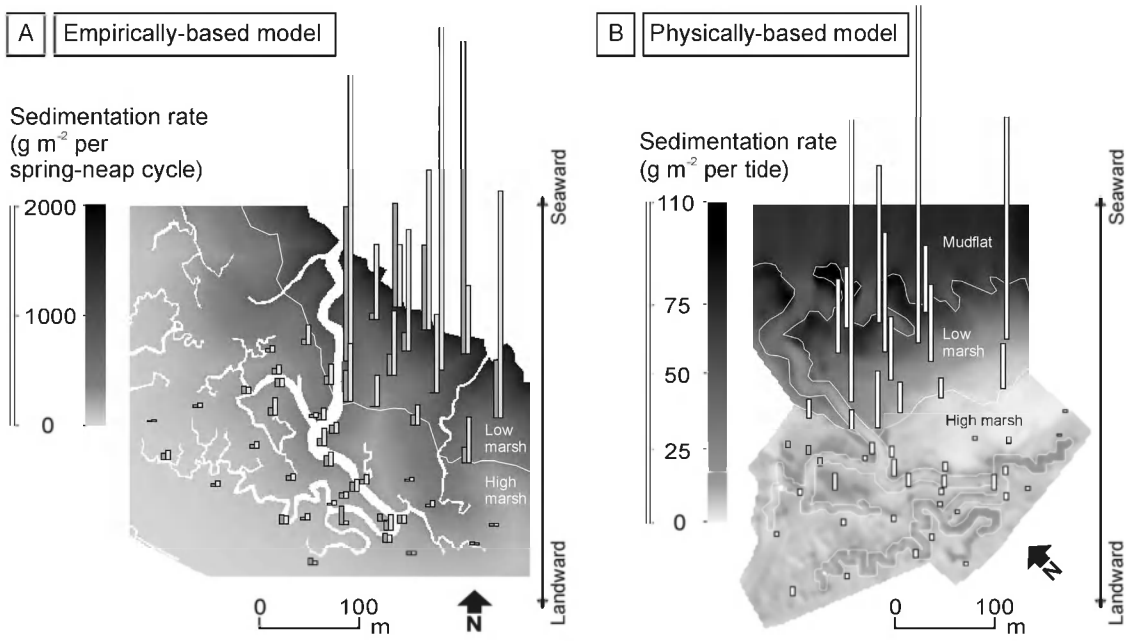

Figure 3. Example of observed (bars) and simulated (contour maps) spatial sedimentation patterns on a tidal marsh platform (Paulina marsh, SW Netherlands) using (a) the empirically based model of [*Temmerman et al.*, 2003a, 2003b] and (b) the physically based model of *Temmerman et al.* [2005b].

by sediment transport and deposition, such as the fluxes of organic matter, nutrients, contaminants, and seeds [e.g., *Struyf et al.*, 2007].

[9] All existing models of sediment fluxes in salt marshes assume that tidal advection of suspended sediment and sedimentation are the dominant processes, while surface erosion is considered negligible on the marsh platform [e.g., *D'Alpaos et al.*, 2007a; *Temmerman et al.*, 2005b]. Field data have shown that the dense vegetation canopy, which covers the marsh platform, exerts significant friction on the flowing water, thereby limiting peak flow velocities to less than about 0.15 m s^{-1} within the canopy [*Bouma et al.*, 2005a; *Christiansen et al.*, 2000; *Leonard and Luther*, 1995; *Lightbody and Nepf*, 2006; *Neumeier and Ciavola*, 2004], and dissipates wind-driven waves over short distances of a few tens of meters [*Bouma et al.*, 2005b; *Möller et al.*, 1999]. Waves also break or are reflected at the marsh boundary, so that wave energy is limited on the marsh surface [*Fagherazzi and Wiberg*, 2009; *Tonelli et al.*, 2010; *Mariotti et al.*, 2010].

[10] Consequently, bed shear stress levels are generally low on the vegetated marsh platform (<10–4 Pa) [*Christiansen et al.*, 2000]. Furthermore, the roots of salt marsh vegetation strongly increase the shear strength of the sediment bed (up to >4500 Pa) [*Howes et al.*, 2010]. Therefore surface erosion on the vegetated marsh platform is neglected in existing models. Nevertheless, erosion may be observed during extremely high storm surges associated with severe wave conditions [*Howes et al.*, 2010].

[11] Existing models of platform sediment fluxes may be classified into two groups: empirical models and physical models. Empirical models are based on statistical relationships between observed sedimentation patterns and environmental variables (mostly topographical variables) [e.g., *Temmerman et al.*, 2003b]. Physical models have been developed using hydrodynamic and sediment transport equations in order to simulate the flow paths of water and sediment over the platform [e.g., *D'Alpaos et al.*, 2007a; *Rinaldo et al.*, 1999b; *Temmerman et al.*, 2005b]. Here we present examples from both model approaches, focusing on relatively recent spatial models that are two- or three-dimensional, although earlier one-dimensional modeling efforts have also been performed [e.g., *Allen*, 1994; *Woolnough et al.*, 1995].

2.1. Empirical Models of Marsh Sedimentation

[12] Empirical models start from field measurements of spatial sedimentation patterns (Figure 3) followed by statistical analyses in order to relate the observed sedimentation patterns to environmental variables [e.g., *French et al.*, 1995; *Leonard*, 1997; *Temmerman et al.*, 2003a; *Van Proosdij et al.*, 2006]. First, many studies have identified that sedimentation rates decrease with increasing platform elevation [e.g., *Cahoon and Reed*, 1995; *Stoddart et al.*, 1989]. This is simply explained by the fact that lower portions of the marsh platform are flooded more frequently, higher and longer, so that more sediment is supplied and deposited. Second, platform sedimentation rates are found to decrease with increasing distance from tidal channels and from the seaward marsh edge [e.g., *French et al.*, 1995; *Leonard*, 1997; *Reed et al.*, 1999; *Temmerman et al.*, 2003a], which may be explained by progressive sediment deposition along flow paths starting from the channels or marsh edge and directed to the inner portions of the marsh platform [*Christiansen et al.*, 2000]. The underlying mechanism is that suspended sediments start depositing as soon as the flow reaches the marsh platform, where velocities are much smaller than in the

channel [*D'Alpaos et al.*, 2007a]. Sedimentation is also favored by the dense vegetation cover that exerts significant friction and therefore rapidly decreases tidal current velocities and turbulence once the water flows from the channels into the platform vegetation canopy [*Christiansen et al.*, 2000; *Leonard and Luther*, 1995; *Yang*, 1998]. Some field studies have further highlighted the role of vegetation in trapping sediments directly on aboveground plant structures [*Stumpf*, 1983].

[13] On the basis of the above described mechanisms, a spatially explicit empirical sedimentation model has been proposed by *Temmerman et al.* [2003b]. The model describes the spatial variations in platform sedimentation rates using an equation of the form:

$$SR = k.e^{l.H}.e^{m.D_c}.e^{n.D_e} \tag{1}$$

where SR is the sedimentation rate (g m^{-2} per time unit); H is the platform surface elevation (m relative to tidal datum); D_c is the distance to the nearest tidal channel or marsh edge (m); De is the distance to the marsh edge (m) measured along the nearest creek; and k, l, m, and n are model coefficients for which $k > 0$ and l, m, $n < 0$. Values of k, l, m, and n are estimated by multiple nonlinear regression fitting of equation (1) through an empirical data set of SR, H, D_c, and D_e values. Equation (1) is then spatially implemented on a regular rectangular grid. For each grid cell, H must be calculated from a digital elevation model, and D_c and D_e are calculated from a remote sensing image from which the tidal channel network and marsh edge are extracted. Most GIS software programs offer algorithms to do this [see, e.g., *Temmerman et al.*, 2003b]. Figure 3a shows an example of the spatial implementation of this model for a specific tidal marsh, illustrating that observed sedimentation patterns are reasonably well reproduced [*Temmerman et al.*, 2005a].

2.2. Physical Models of Marsh Sedimentation

[14] *Rinaldo et al.* [1999a] were one of the first to propose a set of simplified hydrodynamic equations that describe the two-dimensional depth-averaged flow field over a tidal marsh platform. Their model basically assumes that the tide propagates instantaneously (i.e., by immediate vertical adjustment of a flat water surface) through the tidal channel network dissecting the marsh platform, and that the flow on the marsh platform is dominated by a balance between water surface slope and friction. It is further assumed that the marsh platform is flat, that the friction is constant in space and time, that spatial variations in water surface above the platform are much smaller than the average water depth, and that the length of the marsh platform is much smaller than the tidal wavelength. Under these assumptions, *Rinaldo et al.* [1999a] reduced the shallow water equations to a Poisson approximation of the form [see *Rinaldo et al.*, 1999a; *Fagherazzi et al.*, 2003]:

$$\nabla^2\eta_1 = \frac{\lambda}{{D_0}^2}\frac{\partial\eta_0}{\partial t} \tag{2}$$

where η_1 is the local deviation of the water surface from its instantaneous average value, η_0; λ is a constant bottom friction coefficient; and D_0 is the average water depth above the platform. This model is used to calculate water surface slopes above the marsh platform at any time during a tidal cycle and to derive flow directions at any location above the platform following the direction of steepest water surface slope. Depth-averaged flow velocities are calculated from

$$\nabla\eta_1 = -\frac{\lambda}{D}U. \tag{3}$$

The model of *Rinaldo et al.* [1999a] has been used in later publications to address several aspects of tidal marsh morphodynamics, including the transport and deposition of suspended sediments on the marsh platform [*D'Alpaos et al.*, 2007a]. Suspended sediment transport may be generally modeled by an advection–diffusion equation of the form:

$$\frac{\partial(CD)}{\partial t} + \nabla.(UCD - k_D D\nabla C) = E - S \tag{4}$$

where C is the depth-averaged suspended sediment concentration; D is the local water depth; U is the local depth-averaged flow velocity field; k_D is a diffusion coefficient; E is the local erosion rate; and S is the local sedimentation rate. For cohesive sediments, E and S are generally modeled as [*Partheniades*, 1965]

$$E = E_0\left(\frac{\tau}{\tau_e} - 1\right) \text{for} \tau > \tau_e \tag{5}$$

$$S = w_s C\left(1 - \frac{\tau}{\tau_s}\right) \text{for} \tau < \tau_s \tag{6}$$

where τ is the local bed shear stress; τ_e is the critical bed shear stress for erosion (E = 0 when $\tau < \tau_e$); E_0 is an empirical erosion coefficient; τ_s is a critical bed shear stress for sedimentation ($S = 0$ when $\tau > \tau_s$); and w_s is the settling velocity of the suspended sediment. On a vegetated marsh platform, $\tau < \tau_e$ in most cases, so that erosion may be neglected.

[15] *D'Alpaos et al.* [2007a] simulated the transport and deposition of suspended sediment on a marsh platform assuming that the tidal channels are the sources of the suspended sediment. Their model results basically show that simulated sedimentation patterns are governed by a decrease in sedimentation rate with increasing distance from the channels, as a consequence of progressive sediment settling along simulated flow paths that are more or less perpendicular to the channels.

[16] While the simplified hydrodynamic scheme of *Rinaldo et al.* [1999a] and *D'Alpaos et al.* [2007a] assumes that virtually all water and sediment is supplied to the marsh platform through the channels, field data have shown that considerable water volumes (up to 60% of total volume) are directly transported as sheet flow from the marsh edge [*French et al.*, 1995; *Temmerman et al.*, 2005a]. Field data

further show that the partitioning of flow through the channels versus flow over the marsh edge is controlled by the depth of flooding of the marsh platform. The deeper the marsh platform and its vegetation canopy are submerged, the greater the percentage of water that flows over the marsh as sheet flow rather than through the channels [*Temmerman et al.*, 2005a]. Therefore the hydrodynamic scheme of *Rinaldo et al.* [1999a] and *D'Alpaos et al.* [2007a] is better suited to capture the initial stages of the marsh flooding and drainage, when the water depth on the platform is small. Since the peaks in channel velocity are reached around bankfull [*French and Stoddart*, 1992], this scheme provides excellent estimates of the formative discharge in the channel network.

[17] Platform flow directions may also considerably change during single tides, and these changes seem to occur around the moment of submergence of the microtopographic relief or submergence of the vegetation canopy [*Christiansen et al.*, 2000; *Davidson-Arnott et al.*, 2002; *Torres and Styles*, 2007].

2.3. Coupling Vegetation and Marsh Sedimentation

[18] *Temmerman et al.* [2005b] presented a physically based model approach accounting for the interacting effects of inundation depth, vegetation canopy structure, and platform microtopography. They combined the three-dimensional hydrodynamic model Delft3D with a sediment transport model in presence of vegetation [*Nepf*, 1999]. In contrast to the work of *Rinaldo et al.* [1999a], this hydrodynamic model does not assume instantaneous vertical adjustments of a flat water surface in the tidal channels; instead the model explicitly simulates the interactions of tidal propagation through the channels and over the platform. The model of *Rinaldo et al.* [1999a] is therefore ideal in situations where a small tidal excursion and limited water depths on the marsh platform result in a simplified system behavior. On the other hand, high rates of change of tidal level give rise to a complex hydrodynamics characterized by sheet flow over the marsh platform and relevant fluxes from the marsh boundaries.

[19] An important aspect of the model is that it accounts for the influence of the vegetation canopy on the vertical profile of the velocity and related drag, adding an extra source term of friction force, $F(z)$, caused by rigid vertical plant structures, to the momentum equations:

$$F(z) = 0.5\rho_0\phi(z)n(z)|\mathrm{U(z)}|\mathrm{U(z)} \tag{7}$$

where ρ_0 is the fluid density; $\Phi(z)$ is the diameter of plant structures at height, z, above the bottom; $n(z)$ is the number of plant structures per unit area at height z; and $U(z)$ is the horizontal flow velocity at height z. The model further includes turbulence effects of the vegetation canopy.

[20] The turbulence closure used in this model is a classical k-ε model, which is then modified to include extra source terms for k (turbulent energy generation) and for ε (turbulent energy dissipation) as a consequence of the vegetation. The extra source terms for k and ε are dependent on vegetation parameters such as the diameter of the stems and spacing in between the stems. The closure scheme was calibrated to measured turbulence data from a laboratory flume experiment with vegetation [see *Bouma et al.*, 2007].

[21] It is important to stress that nonlinear friction due to vegetation is a very complex process, and equation (7) is just a simplified approximation trying to account for the presence of plant structures on the marsh platform.

[22] The model of *Temmerman et al.* [2005b] showed that the vegetation canopy has a crucial impact on the spatial flow and sedimentation patterns in a tidal marsh, while the influence of the platform microrelief (around 0.3 m) is minimal. When vegetation is considered, the simulated tidal flow is concentrated toward the channels, because friction is much lower in the bare channels than on the densely vegetated platform. Consequently, flood flow velocities are much higher in the channels ($\sim$0.6 m s^{-1}) than on the vegetated platform ($\sim$0.1 m s^{-1}). Given the size of the channels and their spacing on the marsh platform, most of the tidal flow rate is carried through the channels. Hence the platform is flooded from the channels with flow directions more or less perpendicular to the channel edges. In accordance with this flow pattern, simulated sedimentation rates decrease with distance from the channel edges (Figure 4b). Therefore, for vegetated marsh surfaces, the simplified model of *Rinaldo et al.* [1999a] is an excellent approximation of tidal hydrodynamics. In contrast, when vegetation is assumed to be absent, the flow is less concentrated in the channels, so that the speed of flood propagation through the channels and over the platform is comparable, and the platform is flooded in part from the seaward marsh edge. Consequently, simulated sedimentation patterns on the platform also depend on the distance from the marsh edge, leading to channel infilling (Figure 4c). *Temmerman et al.* [2005b] conclude that the presence of marsh vegetation has a profound impact on (1) the development of natural levees along channels and (2) the maintenance and even formation of dense channel networks [see also *Temmerman et al.*, 2007].

[23] *Temmerman et al.* [2005b] further explain the occurrence of changes in platform flow directions during a single tidal cycle, as a consequence of gradual submergence of the vegetation canopy. At the onset of platform flooding, flow directions are always perpendicular to the channels. However, as the vegetation canopy is submerged, the relative difference in friction between the channels and platform decreases, so that larger-scale sheet flow from the marsh edge onto the platform becomes increasingly important. The model simulations show that this partitioning of flow through channels versus over the marsh edge is strongly controlled by inundation depth and by the height and density of the vegetation canopy. With larger inundation depths, the percentage of water that is supplied through the channels decreases, and that is why distance from channels plays a minor role in explaining sedimentation patterns on low-lying marshes [*Temmerman et al.*, 2005a]. Furthermore, the taller and denser the vegetation canopy, the more water that is supplied through the channels, which results in stronger

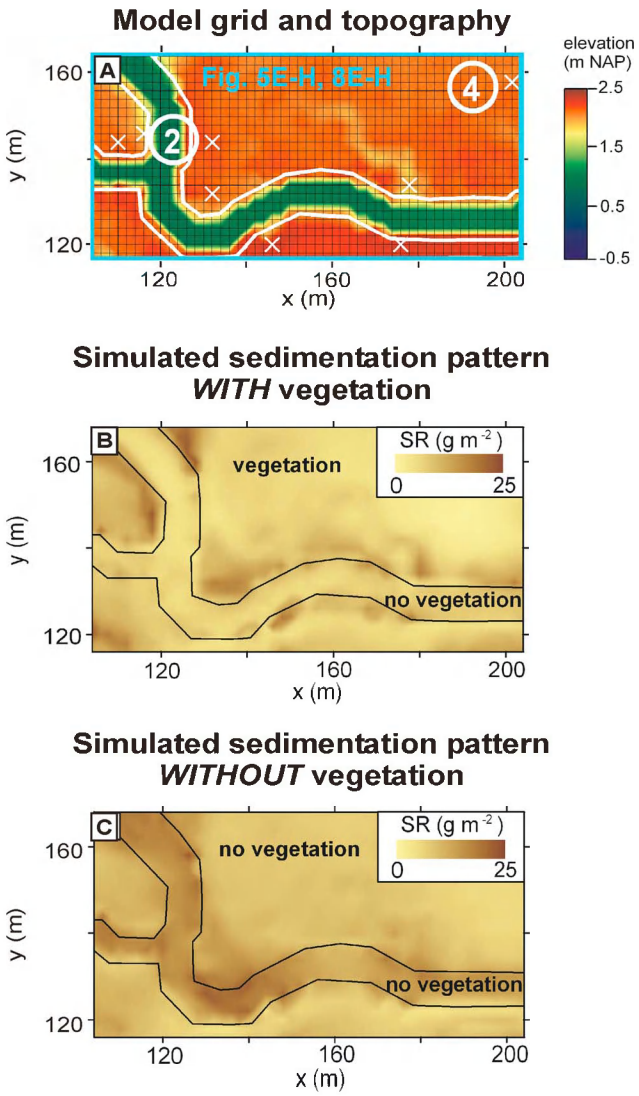

Figure 4. Simulations of flow and sedimentation patterns on a tidal marsh with the model Delft3D. A detail of the model domain is shown, representing a marsh platform dissected by a tidal channel. (a) Model grid and input topography. (b) Sedimentation pattern after one tide with presence of vegetation on the marsh platform. (c) Sedimentation pattern after one tide without vegetation on the marsh platform (modified from *Temmerman et al.* [2005b]).

sedimentation gradients with distance from the channels [*Temmerman et al.*, 2005b].

[24] The model of *Temmerman et al.* [2005b] only considers rigid vegetation elements, when in reality vegetation is flexible and thus gives rise to complex interactions between flow and vegetation structures. Furthermore, the complex vertical structure of real vegetation is neglected. In fact, marsh vegetation may be less dense at low height, where the main stem is located, and denser where the plant structure branches out. This complex biomass distribution creates equally complex effects, producing frictional forces which are a function of the water level.

[25] Moreover, this model is hydrostatic and does not capture the full 3D hydrodynamics. Finally, the assumption of fully developed turbulent flow given the quadratic dependence on velocity might be unrealistic for the entire tidal cycle, since the velocities over the marsh are such that the flow during slack water is likely in transition between a viscous and a turbulent regime.

3. MODELING MARSH BOUNDARY EVOLUTION

[26] Salt marshes develop in intertidal zones when conditions are sufficiently benign to allow for plant growth. When sediment supply is sufficient, salt marsh vegetation can accumulate extensive amounts of fine-grained sediment, which can result in the formation of a salt marsh plateau [*Allen*, 1989]. Consolidation of clays and silts on this plateau is strengthened by the rooting activities of the vegetation. Higher elevation and sediment stability improve plant growth, resulting in a positive feedback between increased sedimentation and increased plant growth.

[27] Because the remaining tidal flat is not accumulating sediment in equal amounts, the edge between the salt marsh and the tidal flat becomes increasingly steep and vulnerable to wave attack. This can cause the formation of strongly erosive marsh cliffs, which capture large amounts of wave energy as they are often near vertical. The combined effects of increased consolidation and direct protection by vegetation maintain a steep cliff that moves inland along a prolonged front (Figure 5). The front can be maintained for decades and destroy extensive areas of salt marsh as it translates landward [*Van der Wal et al.*, 2008]. This process is a consequence of the inevitable increase in elevation of the marsh relative to the surrounding tidal flat and is crucial for understanding marsh dynamics [*Van de Koppel et al.*, 2005]. Moreover, external forcing like large storms, sea level rise, and variations in sediment supply can strongly determine the evolution of the marsh scarp and influence the coupling between vegetation dynamics and morphology [*Mariotti and Fagherazzi*, 2010].

[28] Current research provides information that can be used to distinguish between endogenous and exogenous causes of marsh erosion. In locations where cliff erosion is an endogenous process, the tidal flat sometimes reemerges in front of the cliff, becoming again suitable for plant growth. This has been observed in a number of marshes along the Westerschelde Estuary, Netherlands [*Van de Koppel et al.*, 2005; *Van der Wal et al.*, 2008]. Thus the dynamics of vegetation patches in front of actively eroding salt marsh cliffs can be used as indicators of endogenous marsh erosion. Moreover, as young salt marsh vegetation can be (but not always) more diverse than the older marsh plateau, cliff erosion can be interpreted as complex natural dynamics that leads to salt marsh rejuvenation, thus maintaining structural and species biodiversity in salt marsh ecosystems.

[29] *Mariotti and Fagherazzi* [2010] presented a one-dimensional numerical model for the coupled long-term evolution of salt marshes and tidal flats. The model focuses on the migration of the boundary between the two landforms as a function of wind waves, sediment erosion, and deposition, as well as the effect of vegetation on sediment

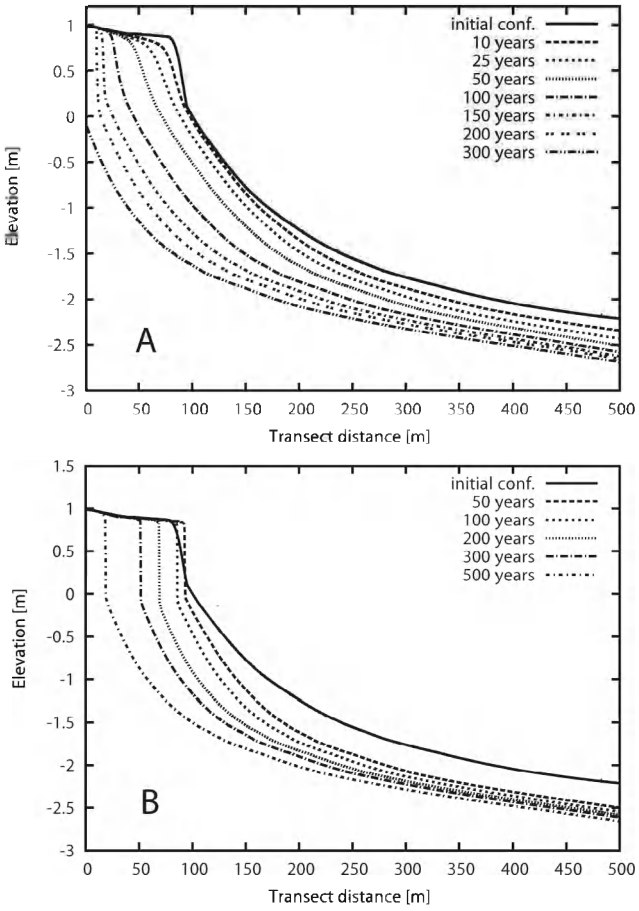

Figure 5. Erosion of a salt marsh boundary simulate with the model of *Mariotti and Fagherazzi* [2010]. The evolution of the profile starts from a fully developed salt marsh, imposing a sediment concentration equal to 0.1 g L^{-1} at the seaward boundary. (a) Without vegetation. (b) With vegetation [after *Mariotti and Fagherazzi*, 2010].

dynamics. Numerical simulations demonstrate that a vertical marsh slope forms during marsh retreat and that vegetation determines the rate of marsh progradation and regression (Figure 5). *Mariotti and Fagherazzi* [2010] relate the erosion of the marsh boundary to wave characteristics by

$$R = \begin{cases} 0 & P < P_{cr} \\ \beta(P - P_{cr}) & P > P_{cr} \end{cases} \quad (8)$$

where R is the rate of boundary erosion; P is the wave power per surface unit dissipated by breaking at the marsh boundary; and P_{cr} is a threshold value for erosion, below which the waves are unable to affect the scarp. In this model the effects of vegetation roots and sediment characteristics on the erodibility of the marsh boundary are not described in detail but included in the β parameter. While vegetation clearly reduces the height and erosive power of waves propagating inland [*Le Hir et al.*, 2007; *Gedan et al.*, 2011], *Feagin et al.* [2009] argue that vegetation does not have a major effect on the erodibility of the marsh margin to wave impact. However, vegetation might dictate the style of boundary erosion, favoring the formation of a steep scarp, undercutting, and cantilever or toppling failure.

[30] *Tonelli et al.* [2010] used a numerical model solving the coupled Boussinesq-nonlinear shallow water equations to evaluate the effect of wave action on marsh boundaries as a function of tidal elevation and wave height. Results show that the wave thrust on the marsh scarp strongly depends on tidal level. The thrust increases with tidal elevation until the marsh is submerged and then rapidly decreases. Therefore, when the marsh is flooded, waves affect the marsh boundary less, and the maximum lateral erosion occurs when the water elevation is just below the marsh platform.

[31] Marsh cliff movements have also been shown to be independent of wave action, with debris that collects and stabilizes the cliff during periods without waves. Often sediments fill the spaces between blocks toppled or slumped from the scarp, forming a gentle slope [*Allen*, 1989].

[32] The effect of increased sea level on the dynamics of salt marsh edge erosion is still unknown. The amount of wave energy that can reach the edge of the cliff is determined to a large extent by the depth and slope of the tidal flat that often exists in front of a (sedimentary) marsh. Sea level rise will increase the relative depth of this tidal flat, and hence more wave energy will be imposed upon the salt marsh edge. Moreover, as the water level increases, it will become increasingly difficult for new vegetation to establish on the tidal flat that is exposed by the retreating edge [*Fagherazzi and Wiberg*, 2009; *Mariotti et al.*, 2010].

[33] Simulations carried out by *Mariotti and Fagherazzi* [2010] indicate that a low rate of sea level rise increases wave dissipation and sediment deposition while a high rate of sea level rise leads to wave erosion and regression of the marsh boundary (Figure 6). Hence, there is the possibility that edge erosion becomes more severe, and recovery is hampered, by sea level rise, further squeezing salt marshes between increased human occupation at the landward side, and increased sea level at the estuarine side. More research is clearly needed to address this important point.

4. DYNAMICS OF MARSH CHANNELS

[34] A large body of literature exists describing salt marsh channel initiation and development [e.g., *Yapp et al.*, 1916, 1917; *Pestrong*, 1965; *Redfield*, 1965, 1972; *Beeftink*, 1966; *Gardner and Bohn*, 1980; *French and Stoddart*, 1992; *Steel and Pye*, 1997], the hydrodynamics of salt marsh channels [e.g., *Boon*, 1975; *Pethick*, 1980; *French and Stoddart*, 1992; *Rinaldo et al.*, 1999a, 1999b; *Temmerman et al.*, 2005b; *Fagherazzi et al.*, 2008], and their morphometric features [e.g., *Fagherazzi et al.*, 1999; *Rinaldo et al.*, 1999a, 1999b; *Marani et al.*, 2003; *Novakowski et al.*, 2004; *Feola et al.*, 2005; *Marani et al.*, 2006]. In spite of their fundamental role in the ecomorphodynamic evolution of salt marsh systems, only in the last few years have numerical models been developed to describe the morphogenesis and long-term dynamics of salt marsh channels [e.g., *Fagherazzi and Furbish*, 2001; *Fagherazzi and Sun*, 2004; *D'Alpaos et al.*, 2005, 2006; *Marciano et al.*, 2005; *Perillo et al.*, 2005; *Minkoff et al.*, 2006; *Kirwan and Murray*, 2007; *Temmerman*

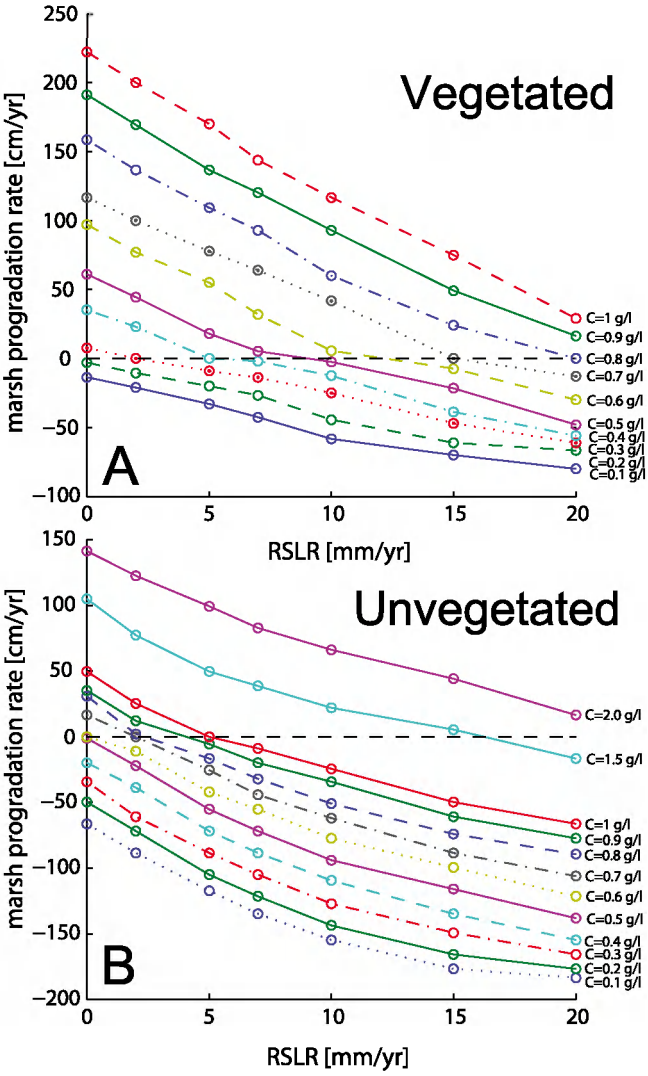

Figure 6. Progradation and erosion rates of the marsh boundary computed with the model of *Mariotti and Fagherazzi* [2010] as function of RSLR and sediment concentration. Positive values indicate progradation, and negative values indicate erosion. (a) With vegetation. (b) Without vegetation [after *Mariotti and Fagherazzi*, 2010].

et al., 2007]. In one isolated case, the initiation and evolution of tidal channel networks have been described in the framework of a scaled laboratory model [*Stefanon et al.*, 2010]. Although recent studies have helped refine our understanding of salt marsh channel dynamics, the dominant mechanisms and chief processes governing the initiation and development of these fundamental geomorphic features of the tidal landscape are not completely understood and still under debate. Moreover, more research is needed to quantify the sensitivity of the models to inevitable errors in the description and sediment transport processes, and how these errors might affect morphological predictions.

4.1. Tidal Channel Initiation and Development

[35] It is generally agreed that the incision and subsequent elaboration of a channel network on a tidal platform is one of the chief morphological processes involved in the evolution of the tidal landscape. Tidal channel initiation can be ascribed to the concentration of tidal fluxes over a surface, which could be a sand or mudflat, or a terrestrial region that has been encroached by salt water due to sea level rise or breach opening on a littoral barrier. The concentration of tidal fluxes over the surface, possibly induced by the presence of small perturbations of bottom elevations, produces local scour as a consequence of the excess bed shear stress, thus favoring the initiation of drainage patterns characterized by shelving banks (see, e.g., Figure 7). Tidal fluxes further concentrate within the forming channel due to its increasing cross-sectional area and decreasing flow resistance as a result of the increase in the depth of flow within the channel [*Fagherazzi and Furbish*, 2001]. The increased flow velocity associated with reduction of the relative bottom roughness in the channel with respect to the adjacent marsh platform leads to higher bottom shear stresses and channel erosion. Consequently, erosion and deepening of the channel creates a positive feedback mechanism between erosion and channel formation which leads to the development of the incised tidal patterns.

[36] The above described mechanism of channel initiation and development is outlined by observational evidence and by a number of conceptual and numerical models [e.g., *Beeftink*, 1966; *French and Stoddart*, 1992; *Fagherazzi and Furbish*, 2001; *D'Alpaos et al.*, 2006; *Temmerman et al.*, 2007]. During the earlier stages of the evolution of tidal

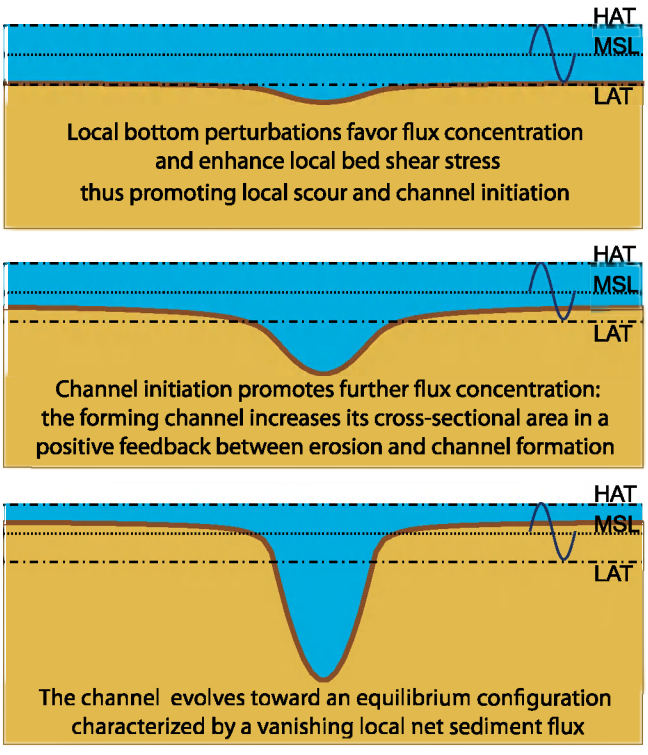

Figure 7. Sketch of the process of channel formation starting from a nearly flat bottom configuration. Small perturbations of bottom elevations enhance flux concentration, leading to bottom erosion and the initiation of a channel in which tidal fluxes further concentrate, thus increasing channel dimensions in a self-sustained process.

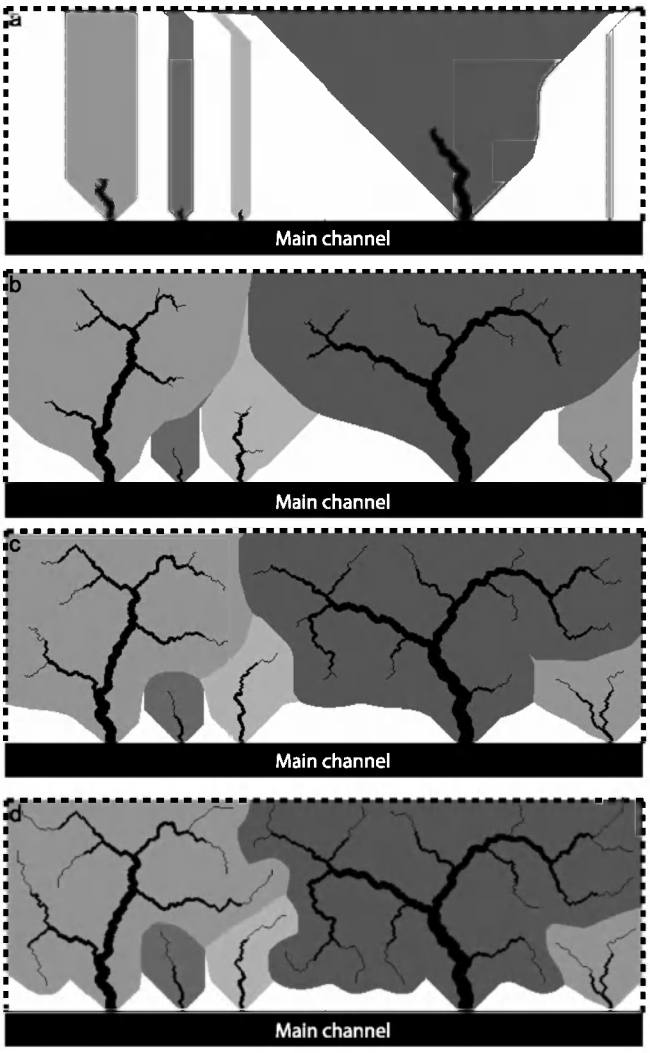

Figure 8. Time evolution of planar network configurations and related watersheds within an ideal rectangular domain limited by a main channel at the bottom and by otherwise impermeable boundaries (dashed lines). Snapshots represent the evolution in time of the creek networks obtained after (a) 20, (b) 200, (c) 600, and (d) 1000 model iterations. Shaded areas represent the watersheds associated to the forming creek networks; the portion of the domain in white is drained by the boundary channel at the bottom side (adapted from *D'Alpaos et al.* [2009]. Copyright Elsevier 2009.)

channels, the tidal network develops via headward growth and tributary initiation through the carving of incised cross sections, where the local shear stress exceeds a critical shear stress for erosion. As the channels evolve and progressively drain larger portions of the marsh landscape and therefore capture a larger tidal prism, their cross-sectional areas expand to accommodate the increasing discharge.

[37] Field observations and related conceptual models describing the coupled evolution of salt marshes and channel networks support the above scenario [e.g., *D'Alpaos et al.*, 2005; *Kirwan and Murray*, 2007; *Temmerman et al.*, 2007]. As an example, Figure 8 shows some snapshots of the progressive development of salt marsh channels obtained by using the morphodynamic model of *D'Alpaos et al.* [2005] that is based on the simplified hydrodynamic model proposed by *Rinaldo et al.* [1999a, 1999b] (see section 2.2) which reduces the two-dimensional shallow water equations to a Poisson boundary value problem. The channels cut through an idealized rectangular domain, limited by impermeable boundaries on the top and on the lateral sides and flanked by an existing channel on the bottom side. Small incisions are initiated at sites along the bottom channel and then progressively grow because of the increase in flowing discharges enhanced by network development at sites in which the local bottom shear stress, controlled by water surface gradients, exceeds a threshold value for erosion. The model reproduces several observed characteristics of real tidal networks; however, the simulated channels are only statistically similar to natural ones [*D'Alpaos et al.*, 2005]. In fact, only statistical parameters like drainage density, unchanneled length, and area probability distributions are correctly reproduced, whereas the exact location of each tidal channel can vary from simulation to simulation.

[38] The dynamics of the system is characterized by a competition among developing networks to capture the available watershed area, by the scouring of the channel cross sections due to the action of the flowing discharges, and by the feedbacks between network expansion and discharge concentration at the tips of the network. Similar results have also been obtained by *Fagherazzi and Sun* [2004] and *Kirwan and Murray* [2007] utilizing process-oriented models that account for the role of local gradients of a Poisson-parametrized water surface [*Rinaldo et al.*, 1999a], an approach which is particularly suitable for shallow tidal areas of limited extent. *Marciano et al.* [2005] used the Delft3D hydrodynamic model, coupled with sediment transport, to simulate the formation of large-scale tidal patterns in a short tidal basin.

[39] The process of network incision is agreed to be rather rapid: *Steers* [1960] reported a channel headcut growth of up to 5–7 m yr^{-1}, *Collins et al.* [1987] observed a headward erosion of more than 200 m in 130 years, *Wallace et al.* [2005] measured a mean extension rate of 6.2 m yr^{-1}, and *D'Alpaos et al.* [2007b] documented a mean annual rate of headward growth of about 11 m yr^{-1}. After an initial stage of rapid evolution, which gives the network a basic imprinting, the network structure undergoes a slower elaboration and is characterized by the adjustment of channel geometry to variations in the local tidal prism through network contractions and expansions. At equilibrium, the maximum bottom shear produced by tidal currents is just below the critical value for erosion at the channels tips, and therefore the channels do not extend any further. At this point the network displays a distribution of unchannelized lengths with an exponential trend [*D'Alpaos et al.*, 2005, 2007b].

[40] The presence of vegetation may promote channel incision [*D'Alpaos et al.*, 2006; *Temmerman et al.*, 2007] and influence the planimetric evolution of tidal channels because of its stabilizing effects on surface sediments and channel banks [e.g., *Redfield*, 1972; *Garofalo*, 1980; *Gabet*, 1998; *Marani et al.*, 2002; *Fagherazzi et al.*, 2004b; *Kirwan et al.*,

2008]. *Redfield* [1965] reports on changes in tidal channel cross-sectional geometry, through deepening and narrowing, as a consequence of the vertical accretion and horizontal progradation of the adjacent vegetated marsh surface. Such an observation supports the concept of inheritance of the major features of channelized patterns dissecting the salt marshes from previously existing sand or mudflat underlying marsh deposits [e.g., *Redfield*, 1965; *Allen*, 2000; *Marani et al.*, 2003].

[41] Following *Redfield* [1965], *Hood* [2006] proposed a conceptual model of channel growth suggesting that tidal channels might be the result of depositional rather then erosional features, in a rapidly prograding delta. In particular environments (Bahìa Blanca Estuary, Argentina) the interaction between crabs (*Neohelice granulatus*) and halophytic plants (*Sarcocornia perennis*) favors the formation of salt marsh creeks [*Perillo et al.*, 2005; *Minkoff et al.*, 2006]. The bioturbation effects linked to crab-plant interactions exerts, in this case, a relevant role in driving the development of salt marsh creeks, thus overcoming water surface gradients.

4.2. Scaling Properties of Tidal Networks

[42] Tidal networks display basic geometric properties common to natural terrestrial patterns [e.g., *Pestrong*, 1965; *Fagherazzi et al.*, 1999; *Steel and Pye*, 1997; *Novakowski et al.*, 2004] but lack the scale invariance features that are peculiar to fluvial channel networks [*Rinaldo et al.*, 1999a, 1999b; *Marani et al.*, 2003; *Feola et al.*, 2005]. A marked absence of scale-free distributions implies that there is no similarity of the part and the whole within the tidal landscape, in sharp contrast to what happens in fluvial basins where ubiquitous power laws occur [*Rodriguez Iturbe and Rinaldo*, 1997]. This reflects the many conflicting processes acting at overlapping spatial scales that affect the relevant morphodynamics, thus hindering simple geomorphic relationships of the types observed in fluvial basins to hold throughout the actual range of tidal scales. Analyses claiming the contrary may indeed have been misled by the subtleties of network comparisons [e.g., *Novakowski et al.*, 2004]. As pointed out by *Hack* [1957], fluvial basins tend to become longer and comparatively narrower as their size increases:

$$L \sim A^h \tag{9}$$

where A is the total contributing area at any site of a fluvial basin; h is an exponent typically equal to 0.57; and L is the embedded mainstream length, defined as the longest streamwise distance, measured along the network from the outlet to the watershed divide. Hack's law does not seem to be applicable to tidal networks [*Feola et al.*, 2005].

[43] Another relevant morphological measure is introduced by computing the downstream unchannelled length, ℓ, evaluated along the flow streamlines determined through the steepest descent direction of the water surface from every salt marsh site to the nearest channel [*Marani et al.*, 2003]. The properties of the probability density function of this length, ℓ, are physical indices of network capability to drain the basin and thus provide an appropriate definition of drainage density. A clear tendency to develop watersheds described by exponential decays of the probability distributions of unchanneled lengths has been observed for about 140 watersheds within 20 salt marshes in the lagoon of Venice, thereby confirming the existence of scale-free features.

[44] Salt marsh channels are also highly sinuous, with meanders that are geometrically similar to their fluvial counterparts [*Marani et al.*, 2002; *Solari et al.*, 2002; *Fagherazzi et al.*, 2004b], although displaying characteristics, such as meander sinuosity, which appear to vary not only from one salt marsh to another, but also within distances of a few hundred meters [*Marani et al.*, 2002]. Strong spatial gradients in discharge favor the development of relevant spatial gradients of characteristic geometric features (e.g., chiefly wavelength and width) whereas the bidirectionality of the discharge shaping the tidal channels often implies a meander evolution that departs from terrestrial meanders [*Fagherazzi et al.*, 2004b]. *Solari et al.* [2002] indicate that tidal oscillations give rise to symmetric oscillations of the point bar-pool pattern around the locations of maximum curvature, without triggering a net migration of the meander if the tide is periodic with zero mean. Moreover, salt marsh channels tend to be characterized by stable planform configurations, with channel migration rates consistently slower than those experienced by fluvial rivers. This is particularly the case of channels cutting through densely vegetated platforms. Dense vegetation, in fact, tends to freeze lateral channel migration while bank undercutting and slumping favors the formation and growth of meanders [*Redfield*, 1972; *Garofalo*, 1980; *Gabet*, 1998; *Marani et al.*, 2002; *Fagherazzi et al.*, 2004b]. Block collapse through a combination of cantilever and toppling failures produces bank migration [*Allen*, 1989], whereas the persistence of failed bank material, which temporarily protects the bank from erosion, decreases the rates of lateral migration [*Gabet*, 1998].

5. COUPLING VEGETATION AND SEDIMENTARY PROCESSES IN SALT MARSHES

[45] Salt marsh macrophytes maintain the elevation of marshes by trapping inorganic sediments [e.g., *Gleason et al.*, 1979; *Leonard and Luther*, 1995; *Li and Yang*, 2009] and through direct deposition of organic sediments [e.g., *Turner et al.*, 2001; *Nyman et al.*, 2006; *Langley et al.*, 2009; *Neubauer*, 2008]. Both trapping and organic deposition is positively correlated with plant biomass [e.g., *Gleason et al.*, 1979; *Li and Yang*, 2009; *Morris et al.*, 2002], which is controlled, in part, by the elevation of the marsh platform [e.g., *Morris et al.*, 2002]. Thus there is a strong feedback between the elevation of salt marshes and marsh vegetation (Figure 9).

[46] In salt marsh models all these feedbacks are expressed through process-based equations, which can be implemented in a code using numerical schemes having different levels of approximation and complexity. Here we provide a detailed description of the key equations used for the coupling between vegetation and sedimentary processes.

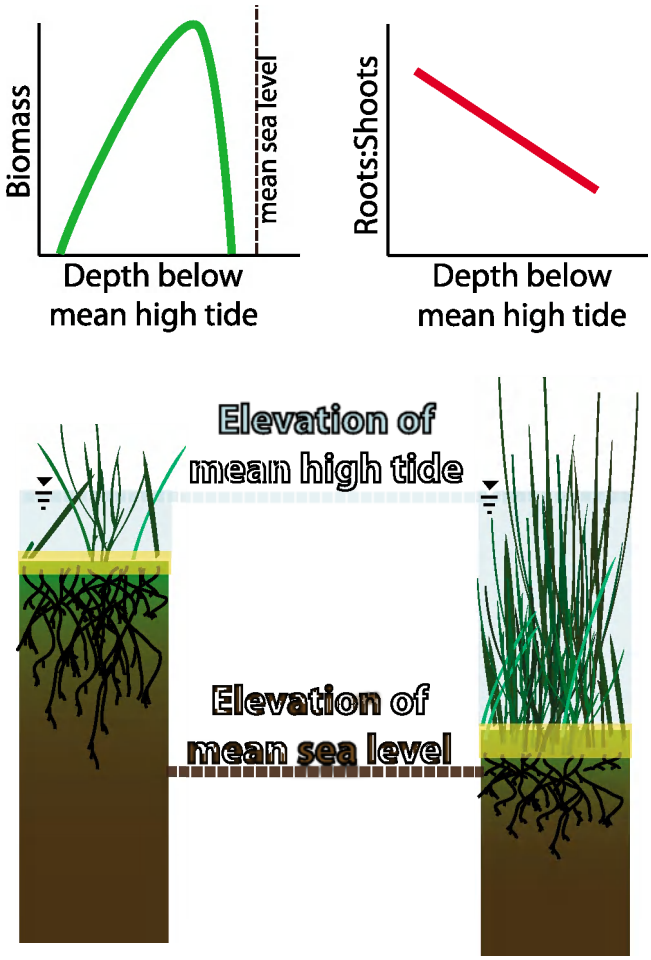

Figure 9. Schematic showing the relationship between mean high tide, biomass, and the roots:shoots ratio. The cartoons are based on measurements at North Inlet, South Carolina [*Morris et al.*, 2002; *Mudd et al.*, 2009].

5.1. Feedbacks Between Marsh Vegetation and Platform Elevation

[47] The biomass of salt marsh macrophytes is a function of a number of factors, including tidal amplitude [e.g., *Kirwan and Guntenspergen*, 2010], latitude, temperature [*McKee and Patrick*, 1988; *Kirwan et al.*, 2009], sediment supply [*Fragoso and Spencer*, 2008], and CO_2 concentration [*Langley et al.*, 2009]. In a single estuary, however, there is typically a distinct elevation range that is occupied by marsh vegetation [e.g., *Redfield*, 1972; *Orson et al.*, 1985; *Morris et al.*, 2005], with marsh vegetation occupying elevations approximately between mean sea level and mean high tide [*McKee and Patrick*, 1988; *Kirwan and Guntenspergen*, 2010] (Figure 9). The biomass and productivity of macrophytes varies strongly within this window [e.g., *Morris et al.*, 2002; *Spalding and Hester*, 2007].

[48] In a given estuary with relatively constant tidal amplitude, temperature, and sediment supply, marsh elevation is the dominant factor in determining plant biomass [e.g., *Morris et al.*, 2002]. For example, *Morris et al.* [2002] found that at North Inlet, South Carolina, *Spartina alterniflora* was most productive at sites 55 cm below mean high tide (in a location where the tidal amplitude was ~60 cm).

[49] Because plants are most productive at some optimum elevation in relation to mean high tide, a negative feedback between plant growth, sea level rise, and sedimentation can occur [e.g., *Morris et al.*, 2002]. If the marsh elevation is lower than the optimum elevation, an increase in the depth of flooding during tides leads to a decrease in plant productivity and therefore a decrease in sedimentation.

[50] On the basis of these observations, *Morris et al.* [2002] put forward the following equation relating standing biomass of halophyte vegetation, B, to the difference between mean high tide and marsh elevation, D:

$$B = aD + bD^2 + c \tag{10}$$

where the parameters a, b, and c depend on vegetation type and marsh location.

[51] This equation provides a simple quantitative feedback between salt marsh ecology (vegetation biomass) and morphology (marsh elevation), and forms the basis for several models of salt marsh evolution [*Mudd et al.*, 2004; *D'Alpaos et al.*, 2005; *Morris*, 2006; *Kirwan and Murray*, 2007; *Mariotti and Fagherazzi*, 2010].

[52] Following this model, an increase in the rate of sea level rise would lead to the drowning of the marsh: eventually the marsh would become too deep for vegetation to survive. *Fagherazzi et al.* [2006] and *Marani et al.* [2007] concluded that this negative feedback is responsible for the bimodal distribution of elevations in typical estuaries with vegetated marshes situated near mean sea level and unvegetated mudflats below.

[53] The model of *Morris et al.* [2002] was derived in tidal marshes dominated by *Spartina* spp. Elsewhere, for example, in Mediterranean and northern European marshes, interspecific competition among numerous halophytic species determines biomass to be an increasing function of elevation [*Marani et al.*, 2004; *Silvestri et al.*, 2005].

[54] For example, *Marani et al.* [2010] use a logistic model for the vegetation biomass:

$$\frac{dB}{dt} = \frac{r(z)B}{d}(d - B) - m(z)B \tag{11}$$

where the biomass $B = pd$ is expressed as the product of vegetation fractional cover, p, and the carrying capacity of the system, d (maximum biomass per unit area); and r and m are the reproduction and mortality rates of the halophytic plants, which depend on the marsh elevation z. By assigning specific functions to r and m the two observed trends of vegetation biomass reaching a maximum for a determined elevation [*Morris et al.*, 2002] or always increasing with elevation [*Silvestri et al.*, 2005] can be simulated within the same framework.

5.2. Inorganic Sedimentation Enhanced by Marsh Vegetation

[55] The presence of plants on the marsh surface can enhance inorganic sedimentation. *Gleason et al.* [1979] measured sedimentation rates as a function of stem density in an

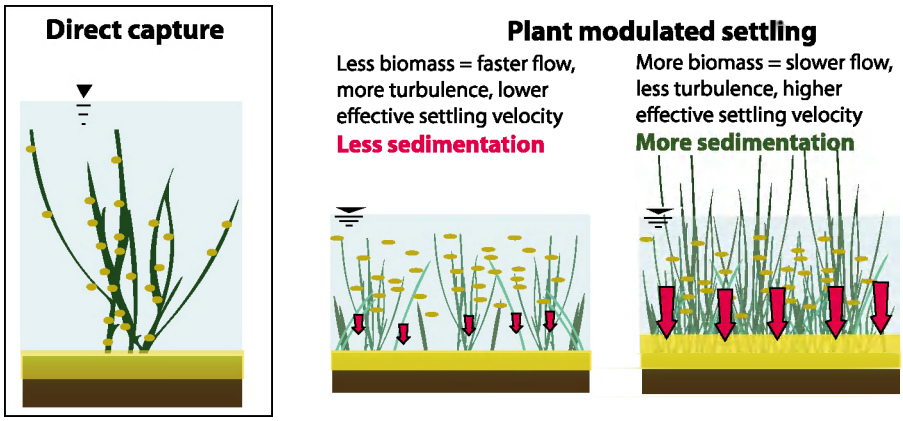

Figure 10. Cartoon showing plants capturing suspended particles and affecting particle settling rates.

experimental apparatus and found that sediment deposition (measured by the total volume of sediment deposited over a fixed number of waves) increased by over 50% if stem density was increased from 27 stems per m^2 to 108 stems per m^2. *Morris et al.* [2002] measured accretion rates on both control and fertilized plots and found that accretion rates on fertilized plots were 0.71 cm yr^{-1} compared to accretion rates of 0.51 cm yr^{-1} on unfertilized plots; fertilized plots had a mean aboveground biomass production of 3280 ± 300 g m^{-2} compared to 780 ± 50 g m^{-2} in control plots. The increase in sedimentation on fertilized plots was entirely due to enhanced inorganic sedimentation brought about by the denser plant canopy. *Morris and Bradley* [1999] found that fertilized sites had lower organic matter content in the top 5 cm of sediment caused by dilution due to increased inorganic sedimentation.

[56] Inorganic sedimentation can occur through natural settling of suspended particles and through the direct capture of particles on plant stems [e.g., *Yang et al.*, 2008] (Figure 10). Particle settling is also closely linked to the marsh plants influence on velocity and turbulence within tidally induced floods. *Leonard and Luther* [1995] measured velocity and turbulent intensity within marsh canopies and found both these quantities reduced with increasing stem densities. *Leonard and Croft* [2006] measured turbulent kinetic energy (TKE) in marsh canopies and found that it decreased with increasing stem density. Similarly, *Neumeier and Amos* [2006] found that TKE was reduced near the marsh surface within vegetated canopies and concluded this would lead to enhanced sedimentation; this result has been corroborated by laboratory studies [*Neumeier*, 2007]. The next generation of salt marsh models should use the data provided by these studies to better reproduce turbulence characteristics in presence of vegetation.

[57] *Nepf* [1999] derived a relationship between TKE per unit mass of water (k), the drag coefficient C_D of emergent vegetation (idealized as an array of cylinders), and the physical characteristics of the marsh vegetation; namely, the stem diameter, d_c, and the projected area of the plants per unit volume, a:

$$K = \alpha_k^2 u^2 (C_D a d_c)^{2/3}, \tag{12}$$

where α_k is a coefficient reported to be 0.9 by *Nepf* [1999] and u is the flow velocity on the marsh. In equation (12) the bulk drag coefficient C_D decreases as the element spacing decreases or ad_c increases, therefore reducing the TKE when a thick vegetation canopy is present.

[58] In fact, the drag coefficient is also related to the characteristics of marsh vegetation. *Tanino and Nepf* [2008] found that the drag coefficient in an array of emergent cylinders can be described as

$$C_D = 2\left(\frac{\alpha_0}{\mathrm{Re}_c} + \alpha_1\right), \tag{13}$$

where α_1 is a function of the solid fraction of stems within the flow. The solid fraction is the area of a single cylinder in cross section times the number of cylinders per unit volume, or $\pi a d_c/4$. The Reynolds number based on the plant stems, $\mathrm{Re_c}$, is a function of flow velocity, the diameter of the stems, and the kinematic viscosity of water: $\mathrm{Re_c} = u d_c/\nu$. The stem diameter and projected area per unit volume of marsh vegetation has been found to follow power law functions of biomass [*Mudd et al.*, 2004, 2010]:

$$a_c = \alpha B^{\beta} \tag{14}$$

$$d_c = \mu B^{\varphi} \tag{15}$$

where B (M L^{-2}) is the biomass per unit area of marsh macrophytes and α, β, μ, and φ are empirical coefficients.

[59] Turbulence helps to maintain particles in suspension so reductions in turbulent kinetic energy may enhance particle settling on salt marshes [e.g., *Leonard and Luther*, 1995; *Nepf*, 1999; *Christiansen et al.*, 2000; *Leonard and Croft*, 2006]. The upward velocity of sediment particles, w_{up}, can be determined by the Rouse equation [e.g., *Christiansen et al.*, 2000; *Orton and Kineke*, 2001]:

$$w_{up} = \kappa_{vk}\sqrt{\frac{\tau}{\rho_w}} \tag{16}$$

where κ_{vk} is von Karman's constant, assumed to be 0.38, τ is the shear stress, and ρ_w is the density of water. Several authors correlated shear stress to total kinetic energy:

$$\tau = \omega k \tag{17}$$

where ω is a constant of proportionality found to vary between 0.19 and 0.21 [*Kim et al.*, 2000; *Soulsby and Dyer*, 1981; *Stapleton and Huntley*, 1995].

[60] Particle settling can then be calculated by subtracting the upward particle velocity caused by turbulence from the settling velocity of particles in still water. Turbulence is produced in stem wakes [*Nepf*, 1999; *Neumeier*, 2007], but this is counteracted by a reduction in velocity due to increased drag. The net effect of denser vegetation is to reduce turbulent kinetic energy [e.g., *Mudd et al.*, 2010].

[61] Particles suspended in tidal waters can also be captured directly by plant stems and leaves [e.g., *Palmer et al.*, 2004; *Li and Yang*, 2009]. *Li and Yang* [2009] measured particle capture on a *Spartina alterniflora* marsh near Shanghai, China, and found it to increase with increasing stem density. *Palmer et al.* [2004] conducted laboratory experiments and determined that particle capture was a function of stem diameter, stem density particle diameter, flow velocity, the concentration of suspended sediment (C), and flow depth. Because stem diameters and stem densities can be related to aboveground biomass (B) [e.g., *Morris and Haskin*, 1990; *Mudd et al.*, 2004, 2010], the rate of mass directly captured by plant stems per unit area of the marsh (Qc) can also be related to biomass and flow characteristics [*D'Alpaos et al.*, 2006; *Mudd et al.*, 2010]:

$$Q_c = \frac{\alpha\kappa}{\nu^{\gamma}} \mu^{\gamma-\sigma} Chu^{1+\gamma} B^{\beta+\varphi(\gamma-\sigma)} d_p^{\sigma}, \tag{18}$$

where h is the flow depth; κ, γ, and σ are empirical coefficients; and d_p is the diameter of suspended sediment particles. Using a numerical model that accounted for both particle capture and enhanced settling due to marsh vegetation, *Mudd et al.* [2010] concluded that in typical marshes (with flow velocities ≤ 0.2 m s^{-1}), settling will dominate inorganic sedimentation.

[62] Currents on the marsh platform are typically too weak to cause erosion [e.g., *Christiansen et al.*, 2000; *Wang et al.*, 1993], but vegetation can focus flow around patches [e.g., *Bouma et al.*, 2009] and in channels [e.g., *Temmerman et al.*, 2005a, 2007], leading to enhanced erosion.

6. MODELING BELOWGROUND ORGANIC PRODUCTION

[63] Plant biomass affects the accumulation of sediments and subsequent salt marsh evolution by trapping mineral and organic particles previously suspended in the water column, by contributing aboveground plant litter to the surface, and by the direct inputs of belowground organic matter as the result of belowground root production, turnover, and decomposition [*Morris and Bowden*, 1986]. Most salt marsh models, however, ignore belowground production.

[64] It is clear that, under certain conditions, belowground production, and subsequent organic matter accumulation, can account for a relatively large fraction of marsh accretion. *Callaway et al.* [1997] measured organic content and ^{137}Cs-derived accretion rates in three *Spartina alterniflora* dominated salt marshes in the northern Gulf of Mexico and found that organic accretion ranged between 7.7% and 21.8% of total accretion (by mass). *Nyman et al.* [2006] found that organic accretion could reach up to 40% of the total accretion rate in *Spartina alterniflora* and *Spartina patens* dominated saltwater sites in Louisiana. *Chmura et al.* [2003] reviewed 24 studies of organic matter accumulation on 85 salt marsh sites across a broad geographic area (the Gulf of Mexico, the northeastern Atlantic, the Mediterranean, the northeastern Pacific, and the northwestern Atlantic) and determined an organic matter accumulation rate as high as 1713 g m^{-2} yr^{-1} at a site in Louisiana.

[65] Despite the relative lack of data, an expanding interest in issues in which belowground processes are critically important (i.e., salt marsh evolution and marsh sustainability in the face of sea level rise) has led to the development of some evolution models that do simulate belowground production. To do so, the modeler is confronted with three challenges: (1) the development of algorithms that describe the rate of belowground production, (2) simulating the distribution of roots within the sediment column, and (3) the development of algorithms that define the rate and proportion of root-derived organic matter that is incorporated into the sediment matrix and contributes to marsh elevation change.

[66] The rate at which dead roots are incorporated into marsh sediments is related to aboveground biomass, and can be stated as

$$M = G - \frac{\partial B_{ag}}{\partial t} \tag{19}$$

where M is a mortality rate in (M L^{-2} T^{-1}); G is a growth rate (M L^{-2} T^{-1}); and B_{ag} is aboveground biomass. Belowground mortality can then be calculated by determining the roots:shoots ratio of the dominant marsh macrophyte under a variety of environmental conditions. *Mudd et al.* [2009] reported that belowground biomass of *Spartina alterniflora* increased with increasing aboveground biomass in North Inlet, South Carolina. In contrast, the roots:shoots ratio at that site was inversely related to aboveground biomass [*Mudd et al.*, 2009] (Figure 9); this relationship could be approximated by a linear function:

$$\frac{B_{bg}}{B_{ag}} = \theta_{bg} D + D_{mbm} \tag{20}$$

where B_{bg} is belowground biomass and θ_{bg} and D_{mbm} are the slope (L^{-1}) and the intercept (dimensionless) of the relationship between the roots:shoots ratio and the depth below MHHW. This relationship is likely site-specific: *Darby and Turner* [2008a, 2008b] found that fertilization of *Spartina alterniflora* in Louisiana resulted in increased aboveground biomass but had no effect on belowground biomass. Because aboveground biomass is related to the elevation of the marsh

platform, this elevation also controls belowground biomass. *Nyman et al.* [2006], for example, found that root growth increased if flooding depth increased, but did not report aboveground biomass at their sampling sites.

[67] Of the salt marsh models that mechanistically simulate belowground production within a sediment column, most [i.e., *Callaway et al.*, 1997; *Rybczyk et al.*, 1998; *Cahoon et al.*, 2003; *Mudd et al.*, 2009; *Kairis and Rybczyk*, 2010] are derivative of *Morris and Bowden*'s [1986] single-year sediment cohort model, originally developed for a freshwater tidal marsh on the North River, Massachusetts. One advantage of the cohort approach is that this framework can simulate the percent sediment organic matter and bulk density with depth, and this output can be compared to actual sediment cores for model calibration and validation. In *Morris and Bowden*'s [1986] original model, simulated live root biomass within a vertical sediment column was assumed to be greatest at the surface and to decrease exponentially with depth and defined as

$$R = R_0\, e^{(-kD)} \tag{21}$$

where R is the root biomass (g cm^{-2}) at depth D (cm); R_o equals the weight of roots at the sediment surface (g cm^{-2}); and k is root distribution parameter (cm^{-1}). The parameter k essentially describes the exponential root distribution with depth (greatest at the surface). The integrated root biomass over all depths is defined as the integral of equation (21):

$$R_i = \int R_0 e^{(-kD)} dD \tag{22}$$

where R_i is defined as the total live root biomass in the soil column (g cm^{-2}). By specifying R_i (usually as a function of aboveground biomass) and assuming that all live belowground biomass is contained with a known rooting depth, one can then use equation (22) to solve for R_o and k [*Morris and Bowden*, 1986].

[68] Labile organic matter, because it decays, does not contribute to marsh accretion, and deposition of low-density, uncompacted organic sediments is offset by compaction. The change in organic carbon can be modeled as

$$\frac{\partial C_l}{\partial t} = -k_l C_l + m\chi_l \tag{23}$$

where the subscript l refers to the labile pool; C (M L^{-3}) is the organic carbon per unit volume; m (M L^{-3} T^{-1}) is the mortality rate per unit volume (M is equal to m integrated over the depth of the rooting zone); k_l is the decay coefficient; and χ_l is the fraction of dead root matter that is labile. Decay rates depend on a number of factors, including (possibly) sulfate concentration and oxygen supply [e.g., *Silver and Miya*, 2001]; many of the factors proposed to control the rate of organic matter decay vary with the depth below the sediment surface. Some authors have suggested depth-dependent decay coefficients [*Conn and Day*, 1997; *Rybczyk et al.*, 1998]. Others, however, have conducted measurements of decay in marsh sediment that show no depth dependence [e.g., *Blum*, 1993].

[69] Compaction can be modeled as [e.g., *Gutierrez and Wangen*, 2005]:

$$E = E_0 - CI \log\left(\frac{\sigma_{eff}}{\sigma_0}\right) \tag{24}$$

where E (dimensionless) is the void ratio; CI (dimensionless) is the compression index; E_0 (dimensionless) is the void ratio at the reference stress, σ_0 (M T^{-2} L^{-1}); and σ_{eff} (M T^{-2} L^{-1}) is the effective stress. The long-term rate of vertical accretion, in units of length per time, is determined by dividing the rate of accumulation of refractory organic material by the density of compacted organic material [e.g., *Mudd et al.*, 2009]. Assuming that all root material is made of refractory carbon and that compressed organic material has a density of 0.1 g cm^{-3}, the maximum vertical accretion rate from organic sediments is approximately 1.7 cm yr^{-1}, based on *Chmura et al.*'s [2003] highest reported organic accumulation rate. *Mudd et al.* [2009], using a model that incorporated compaction, organic decay, and measured productivity and mortality of *Spartina alterniflora* at North Inlet, South Carolina, United States, calculated a theoretical maximum organic accumulation rate of ~2200 g m^{-2} yr^{-1}.

[70] *Kirwan et al.* [2009] found that among North American marshes, Gulf Coast and southwest Atlantic marshes were the most productive, corroborating the results of *Chmura et al.* [2003]. *Kirwan et al.* [2009] estimated that an increase of 4°C could boost productivity by up to 40%, but even if this increase in productivity was mirrored in the production of belowground biomass, this would mean a maximum rate of vertical accretion from organic sediment of 2.4 cm yr^{-1}. This productivity gain could potentially be enhanced because of greater atmospheric CO_2; *Langley et al.* [2009] compared the production of fine roots in plots with ambient CO_2 and plots with CO_2 of ambient +340 ppm and found that fine root production increased by 75% and 35% over two field seasons in the plots with elevated carbon dioxide. Again assuming all of this additional root matter was refractory carbon, and assuming a compacted density of organic matter of 0.1 g cm^{-3}, one could estimate the maximum possible vertical accretion rate due to organic sedimentation as 4.2 cm yr^{-1}. This rate, however, should be considered extreme as organic sediments are highly compressible [e.g., *Mesri et al.*, 1997] and organic material typically contains 20–90% labile carbon, as indicated by the steep decline in organic material content with depth found in virtually all marsh cores [e.g., *Sharma et al.*, 1987].

7. SALT MARSH LANDSCAPE-SCALE ECOSYSTEM MODELING

[71] The objective of an ecosystem-based landscape model is to minimize the computation of physical processes in order to expand the resolution and forecast of the resultant effects on biological systems. Given their relative simplicity, ecosystem-based models can be applied at high resolution to large areas and study the spatial interactions among different ecosystem units. The use of spatially explicit models thus

expands our understanding of geographical and temporal gradients in salt marsh ecosystems [*Fitz et al.*, 1996].

[72] Ecosystem models couple organisms (mainly plants) with their environment by directly or indirectly considering hydrodynamics and water quality parameters (e.g., sediment loads, nutrients, and other biological active particles). Models based on direct calculations simultaneously compute flow, water quality, and biological processes in the same time step. This allows for explicit feedback mechanisms and interactions with results readily available at each time step, but require computational elements of similar size that result in long simulation times. An example of a direct-calculation model is the Coastal Ecological Landscape Spatial Simulation model (CELSS) [*Costanza et al.*, 1990; *Costanza and Ruth*, 1998; *Sklar et al.*, 1985] which includes several environmental forcing (subsidence, sea level rise, river discharge, and climate variability).

[73] Subsequent efforts using the same direct-calculation approach resulted in the Barataria-Terrebonne Ecological Landscape Spatial Simulation model (BTELSS) [*Reyes et al.*, 2000] which focused on historical trends in land loss and habitat change for coastal Louisiana. The BTELSS model consists of an explicit hydrodynamic module with water and particle flow and ecological algorithms modeling critical environmental parameters. For example, the change (p) in plant biomass (B) at a particular cell is computed with the following set of equations:

$$\begin{aligned} \frac{dB}{dt} &= pB \\ p &= P - (\varphi B + \lambda B + \gamma B) \\ P &= \mu P \times F(S \times Z \times T/T_{\max}) \end{aligned} \tag{25}$$

where change in plant biomass is the result of plant production (P) minus changes in biomass due to translocation (φ), litterfall (λ), and respiration (γ) rates; and plant production (P) is calculated synergistically in response to daily salinity (S), flooding (Z), and temperature (T) parameters.

[74] Other direct-calculation ecological models include those of *Martin et al.* [2002] which examined the effects of large fresh water discharges on salt marsh restoration and *Reyes et al.* [2003, 2004a, 2004b] who predicted vegetation responses to the cumulative effects of small river diversions in combination with accelerated sea level rise.

[75] The indirect-calculation models are easier to implement and present substantial decreases in computation time. These models first compute the hydrodynamics and water quality, which are then used to simulate biological processes. Among the most used models based on indirect calculations is the Sea Level Affecting Marshes Model (SLAMM) [*Park et al.*, 1986, 1989; J. Clough and R. A. Park, SLAMM 5.0.2 technical documentation, October 2008, available at http://www.warrenpinnacle.com/prof/SLAMM].

[76] SLAMM is a spatial model that simulates the dominant processes in wetland conversions and shoreline modifications during long-term sea level rise (SLR) and has been used to simulate the effects of accelerated SLR on ecosystem services including biological productivity and water quality improvement of tidal wetlands [*Craft et al.*, 2009]. SLAMM simulates five primary processes that affect wetland fate as sea level rises: inundation, erosion, overwash, salinity, and soil saturation. Model inputs consist of a digital elevation model (DEM), tidal data, rates of wetland vertical accretion, maps indicating the distribution of wetland vegetation, and published predictions of sea level rise [*Church et al.*, 2001].

[77] In addition to submergence, tidal wetlands can undergo habitat conversion as sea level rises and salt water intrudes into brackish and freshwater wetlands, transforming them to more saline marshes. This is important in river-dominated estuaries where the mixing of freshwater and seawater interact to produce a gradient of tidal wetlands, from salt marshes near the open ocean to tidal freshwater marshes and forests in the upper reaches of the estuary. Salt water intrusion is modeled in SLAMM using a "salt wedge" approach based on long-term freshwater discharge and cross-sectional area of the estuary.

[78] Simulation results can be combined with site-(wetland-) specific measurements of ecosystem services to predict how sea level rise will affect delivery of wetland-dependent ecosystem services to coastal landscapes and communities [*Craft et al.*, 2009].

[79] SLAMM was used to simulate the effects of SLR on carbon (C) sequestration and water quality improvement (denitrification) in the Altamaha River Estuary, Georgia, United States. The simulations, using the IPCC A1B mean sea level rise scenario, predict that forest and tidal freshwater marsh will decline by 24% and 38%, respectively, by 2100 (Figure 11). Salt marsh is predicted to decline by 8% whereas brackish marsh area increases by 4%. The model predicts large increases in transitional salt (high) marsh, tidal flat, and estuarine open water as sea level rises. Delivery of ecosystem services related to water quality improvement (denitrification) and carbon (C) sequestration declines as salt marsh is submerged and forest and freshwater marsh convert to brackish marsh habitat.

[80] Overall, in the estuary model, results show that tidal wetland area is reduced by 12%, whereas denitrification and C sequestration are reduced by 10% and 19%, respectively. The disproportionately large decrease in denitrification is attributed to loss of tidal forests which have high rates of denitrification relative to the more saline wetlands. The results of this example illustrate one way of coupling ecosystem-based studies of wetland structure and function with landscape models such as SLAMM to predict how the delivery of wetland ecosystem services will change in response to sea level rise in the coming century.

8. SALT MARSH EVOLUTION AND SEA LEVEL RISE

[81] At the most fundamental level, a marsh must gain elevation at a rate faster than or equal to the rate of sea level rise to maintain its vertical position in the intertidal zone [*Reed*, 1995]. Historically, rates of sediment deposition and organic accretion have been similar to rates of sea level rise in most marshes worldwide. Long-term accretion rates derived from measurements of Pb-210 indicate that sea level rates and accretion rates have been similar over approximately the last century and that accretion rates are fastest in regions with

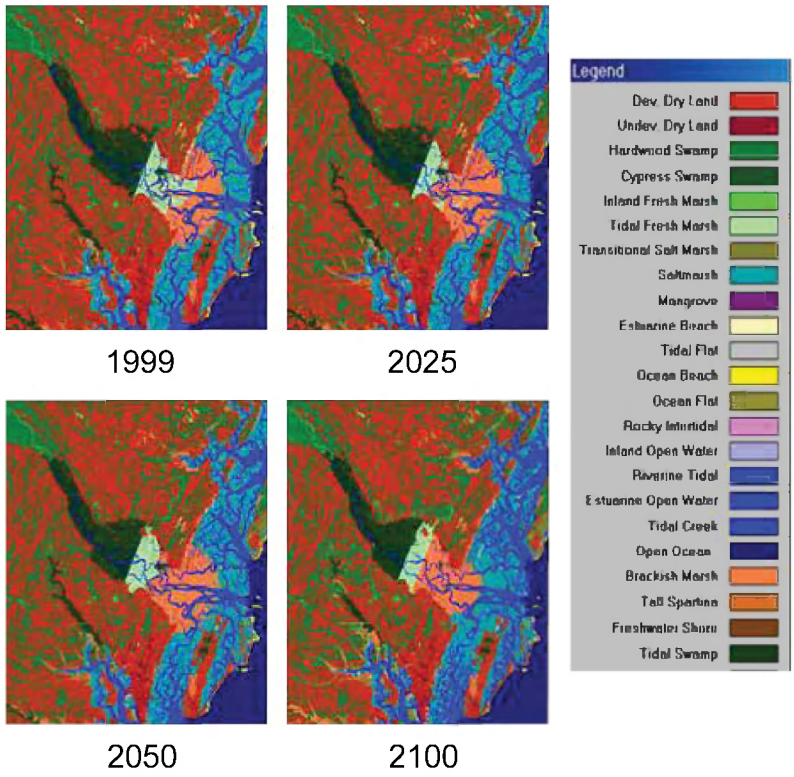

Figure 11. SLAMM simulation of effects of accelerated SLR on tidal marshes of the Altamaha River, Georgia. The simulation was run using the SRES A1B scenario that assumes a 52 cm increase in sea level by 2100. The coarse vertical resolution of the NED data set results in the linear pattern (i.e., striping) of wetland migration observed during the simulation [from *Craft et al.*, 2009]. Used by permission.

rapid sea level rise [*Friedrichs and Perry*, 2001; *French*, 2006]. Direct measurements of elevation change on annual to decadal time scales also suggest a connection between marsh accretion and sea level; most salt marshes and mangroves around the world are accreting faster than or equal to the rate of historical sea level rise plus any local subsidence [*Cahoon et al.*, 2006]. Indeed, sediment cores from many marshes reveal stratigraphic properties that change little over a few thousand years during periods of relatively slow sea level rise [e.g., *Redfield*, 1965].

8.1. Feedbacks Between Accretion, Submergence, and Sea Level Rise

[82] Observations of long-term stability and platform maintenance inspire conclusions that marsh ecosystems must be capable of rapidly adjusting to changes in rates of sea level rise [*Friedrichs and Perry*, 2001]. Several processes, both biological and physical, are likely responsible for the tight coupling between sea level and marsh accretion. From a purely physical perspective, sediment deposition rates on the marsh platform are largely controlled by the duration and frequency of tidal flooding [*Marion et al.*, 2009]. Rates of mineral deposition are highest in low-elevation salt marshes that are inundated for long periods of time and lowest in high-elevation marshes that are periodically flooded [*Pethick*, 1981; *Bricker-Urso et al.*, 1989]. Similarly, rates of deposition at a single location within a salt marsh are highest when tides and inundation depths are highest [*Temmerman et al.*, 2003b]. Therefore, if an increase in the rate of sea level rise is accompanied by more extensive platform flooding, mineral deposition rates will increase. More recent work suggests that this feedback is enhanced by growth characteristics of marsh macrophytes. Long-term measurements of *Spartina alterniflora*, for example, demonstrate that its productivity is strongly correlated to interannual variations in sea level [*Morris et al.*, 2002] and that it grows fastest at relatively low elevations within the intertidal zone [*Mudd et al.*, 2009]. Feedbacks between flooding and accretion are less understood for organic rich marshes, though organic matter decay rates are likely slower in frequently flooded, anaerobic soils. Finally, sediment eroded from one portion of a marsh can be a source of sediment aiding vertical accretion in surviving marshland. For example, eroding marsh edges often have levees just behind the point of wave impact. Similarly, expansion of channel networks in response to accelerated sea level rise may deliver more sediment to portions of the platform that were previously sediment deficient [*D'Alpaos et al.*, 2007a; *Kirwan et al.*, 2008]. These types of ecogeomorphic feedbacks likely explain the persistence of wetlands within the intertidal zone over thousands of years in the stratigraphic record [*Redfield*, 1965] and observations of accretion rates that are highest in regions with historically high rates of sea level rise [*Friedrichs and Perry*, 2001].

[84] Nevertheless, widespread observations of marsh submergence today indicate that there are limits to the ability of ecogeomorphic feedbacks to preserve the position of a marsh

within the intertidal zone. Stratigraphic evidence and tidal gauge records indicate that sea level rise rates were less than 1 mm yr^{-1} for most of the last 2000 years and began accelerating toward modern rates of about 2–3 mm yr^{-1} in the 18th or 19th centuries [*Donnelly et al.*, 2004; *Church and White*, 2006; *Jevrejeva et al.*, 2008; *Gehrels et al.*, 2008]. Perhaps in response, marshes around the world appear to be degrading. The replacement of high marsh vegetation by low marsh vegetation in some salt marshes in New England began at roughly the same time sea level began to accelerate [*Donnelly and Bertness*, 2001]. Marsh elevations appear to be deepening relative to sea level in South Carolina [*Morris et al.*, 2005], channel networks appear to be expanding in South Carolina, New York, and Maryland [*Kearney et al.*, 1988; *Hartig et al.*, 2002; *Hughes et al.*, 2009], and large amounts of marshland are being converted to open water in Louisiana, Maryland, Italy, and southeastern England [e.g., *Reed*, 1995; *Day et al.*, 1999; *Kearney et al.*, 2002; *van der Wal and Pye*, 2004]. In fact, historical rates of marsh loss correlate with historical changes in relative sea level rise rates in coastal Louisiana and the Chesapeake Bay Estuary [*Stevenson et al.*, 1986; *Swenson and Swarzenski*, 1995].

[85] Determining the influence of sea level acceleration remains difficult, however, since the effects of sea level rise alone cannot be isolated in natural wetlands. Sediment supply also exerts a strong control on marsh expansion and decline. A pulse of sediment can lead to a wide range of feedbacks that encourage marsh expansion [e.g., *Mudd*, 2011]. Sediment supply reduction and increased subsidence rates are at least partially responsible for marsh loss in Chesapeake Bay, coastal Louisiana, and Venice Lagoon marshes [*Kearney et al.*, 2002; *Reed*, 1995; *Marani et al.*, 2007]. The main cause of loss of coastal wetlands in the Mississippi Delta is the isolation of the river from the delta trough the construction of levees, which dramatically reduced sediment inputs to the salt marshes [*Day et al.*, 2005]. Moreover, identifying sea level rise as the primary driver of marsh loss is complicated by observations that some marshes are submerging despite vertical accretion rates that exceed relative rates of sea level rise [*Kirwan et al.*, 2008] and that most marshes today have elevations increasing faster than historic rates of sea level rise [*Cahoon et al.*, 2006]. In fact, *Kirwan and Temmerman* [2009] concluded that factors other than historical sea level acceleration were most likely responsible for widespread patterns of marsh submergence.

8.2. Simulating Marsh Evolution Under Sea Level Rise

[86] Numerical models may help determine the direct influence of sea level rise on marsh survival since they offer the distinct advantage of being able to isolate sea level as a forcing variable. Models of platform elevation, for example, show a tendency for marshes to become deeper within the tidal frame in response to an increase in the rate of sea level rise alone [e.g., *French*, 1993; *Allen*, 1995] and can become too deep to support vegetation growth at high rates of sea level rise (i.e., >10 mm yr^{-1}) [*Morris et al.*, 2002]. While these models show vegetated intertidal surfaces to be relatively resilient to changes in sea level, *D'Alpaos et al.* [2007a] suggest that relatively small changes in platform elevation can lead to channel network expansion, and disturbance to vegetation can trigger rapid marsh degradation [*Marani et al.*, 2007; *Kirwan et al.*, 2008].

[87] Although a wide variety of numerical models exists [see also *Kirwan and Temmerman*, 2009, and references therein], most are based on the assumption that marsh accretion rates should increase with inundation due to sea level rise:

$$\frac{dz}{dt} = \frac{k}{z} \tag{26}$$

where dz/dt represents the change in marsh elevation through time (i.e., its accretion rate) and $1/z$ is a proxy for the duration and frequency of inundation. At its most basic level, equation (26) predicts that a decrease in elevation relative to sea level, z, will be accompanied by an increase in the accretion rate. The processes actually responsible for this relationship (implicitly incorporated into k) vary between models and include many of the biological and/or physical feedbacks discussed in earlier sections (e.g., sections 5 and 8.1). In particular, vertical elevation adjustment in most recent models is accomplished primarily through the sedimentation-inundation feedback and the enhanced growth of plants with moderate increases in inundation and its effect on mineral sediment trapping and organic accretion.

8.3. Multiple Stable Equilibria

[88] Several basic patterns evolve out of any model that relies on an inundation-dependent accretion scheme. First, when sea level rise rates are constant a marsh will asymptotically evolve toward an elevation where accretion rates are in equilibrium with sea level. If initial marsh elevations are relatively low (i.e., frequently inundated), accretion is rapid and the surface builds higher in the tidal frame. If marsh elevations are relatively high (i.e., infrequently flooded), accretion is slow, and sea level rise causes the marsh surface to become lower in the tidal frame. *Morris et al.* [2002] explain that the particular equilibrium elevation is controlled by the rate of sea level rise, the amount of sediment available for mineral accretion, and the rate of vegetation growth. Where mineral sediment concentrations decrease with distance from the channel or marsh edge, equilibrium elevations would be expected to decrease toward the marsh interior, resulting in a leveed, gently sloping marsh surface [*Mudd et al.*, 2004]. Conversely, for a marsh dominated by organic accretion, the marsh platform would be expected to evolve toward a flat intertidal surface.

[89] Since marsh elevations evolve toward a condition where vertical accretion balances sea level rise, the equilibrium solution of equation (26) can be rewritten as

$$m = \frac{k}{z} \tag{27}$$

where m represents the rate of sea level rise. Following *Morris et al.* [2002], a change in the rate of sea level rise must be accompanied by a change in marsh elevation. For an acceleration in the rate of sea level rise, the elevation of the

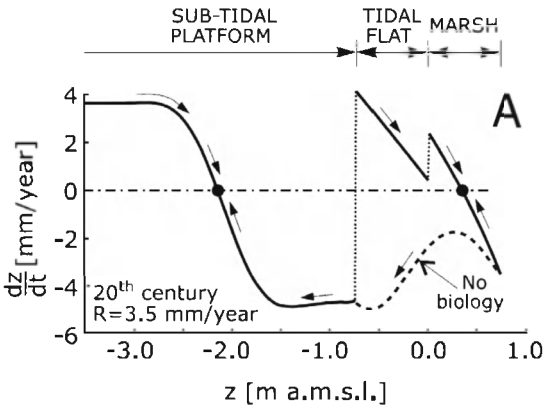

Figure 12. Alternative stable elevations (z) for a hypothetical *Spartina alterniflora* dominated salt marsh under historical rates of sea level rise. Subtidal platform elevations are stable at high rates of RSLR, whereas intertidal elevations are stable at low rates of RSLR. As in the work of *Fagherazzi et al.* [2006], intermediate elevations are unstable and rapidly evolve toward either a high intertidal salt marsh or a bare subtidal flat. The hypothetical case in which no biological activity is present is described by the dashed curve and demonstrates that stable intertidal elevations can only be accounted for with the presence of vegetation. (Figure and caption are from *Marani et al.* [2007]).

marsh (z) must decrease in order to maintain equilibrium. Therefore, at the most basic level, an increase in the rate of sea level rise would be expected to cause an increase in platform flooding as the marsh surface becomes lower relative to sea level. This numerical behavior has been widely observed in field-based studies. *Donnelly and Bertness* [2001], for example, observed that vegetation characteristics of low-elevation marshland replaced high marsh vegetation immediately following the onset of sea level acceleration around 1900 AD. Similarly, elevation distributions at North Inlet appear to indicate a gradually submerging marsh [*Morris et al.*, 2005], while nearby tidal channels are expanding [*Hughes et al.*, 2009].

[90] Of course, imbedded in k, can be many ecogeomorphic feedbacks that are also related to the elevation of the marsh platform and its effect on inundation (see section 5). Plant growth, for example, is a nonlinear function of marsh elevation, where there is an optimum elevation for plant productivity [*Morris et al.*, 2002]. Consequently, models of marsh elevation change that incorporate plant effects have multiple stable equilibria [*Marani et al.*, 2007, 2010] (Figure 12). In particular, the stable equilibrium for an intertidal surface covered by plants is much shallower than the stable equilibrium for a surface where plants are absent. As a result, disturbance to vegetation will tend to promote a transition toward the unvegetated equilibrium state, characterized by a lower elevation relative to sea level and more frequent inundation. At high rates of sea level rise, the equilibrium depth of an unvegetated surface may be subtidal and/or too erosive for vegetation to grow back. In this case, disturbance to vegetation on an otherwise stable intertidal surface would cause a marsh to submerge beyond depths capable of supporting vegetation and therefore shift to an alternative stable state that will never again support plant growth [*Kirwan and Murray*, 2007; *Marani et al.*, 2007; *Kirwan et al.*, 2008].

8.4. Lags Between Sea Level and Morphologic Change

[91] The idea that marshes must become more inundated before they can accrete at faster rates leads to a common observation in numerical experiments that there is a lag between changes in sea level and morphology [*French*, 2006; *Kirwan and Murray*, 2008a; *Kirwan and Temmerman*, 2009; *D'Alpaos*, 2011]. As a brief example, models of salt marsh evolution suggest that in response to a step change in the rate of sea level rise from 1 to 3 mm yr^{-1}, a marsh will lose about 10 cm of elevation relative to sea level before accretion rates equilibrate to the new rate of sea level rise. If sea level is rising at 3 mm yr^{-1}, then in the absence of deposition, it would take 33 years to deepen 10 cm and equilibrate. Of course, the marsh is also building elevation during this time, so the adjustment period (i.e., the lag) is actually much longer ($\sim$100 years) [*Kirwan and Temmerman*, 2009] (Figure 13). As a consequence, marshes are always moving toward, but never reaching, equilibrium with a continuously varying sea level rise typical of real eustatic oscillations [*French*, 2006; *Kirwan and Murray*, 2008a] (Figure 13b). Moreover, simulated marshes never reach equilibrium with a continuously accelerating rate of sea level rise. In scenarios of future acceleration, accretion rates mimic sea level rise rates that occurred about 30–40 years previously [*Kirwan and Temmerman*, 2009] (Figure 13a).

[92] Similar lags between sea level and marsh adjustment will arise in any system where accretion is a positive function of inundation. More detailed analysis suggests that the duration of adjustment is not strongly dependent on the amplitude of sea level change [*Kirwan and Murray*, 2008a; *Kirwan and Temmerman*, 2009]. Abundant sediment availability appears to reduce the lag. Marshes with high mineral sediment inputs adjust more quickly than sediment deficient ones, leading to a spatially heterogenous pattern where marsh areas adjacent to channels adjust quickly to sea level, whereas interior marshland lags behind [*D'Alpaos*, 2011] (Figure 13c).

[93] The temporal lag between sea level change and platform elevation has several implications for interpreting measurements of marsh processes today. First, because the marsh never reaches a stable equilibrium with a continuously oscillating or accelerating rate of sea level rise, measurements of vertical accretion and/or elevation change are highly context dependent. In particular, short-term measurements of elevation change (e.g., from SETs or ^{137}Cs) that are less than the historical rate of sea level rise do not necessarily mean that the marsh is incapable of surviving sea level rise; instead they may simply indicate that a marsh is moving toward a deeper equilibrium [*French*, 2006; *Kirwan and Murray*, 2008a]. Similarly, if we interpret 20th century sea level acceleration as a step change [*Donnelly et al.*, 2004; *Gehrels et al.*, 2008], then observed lags on the order of 50–200 years suggest that marshes have been out of equilibrium with

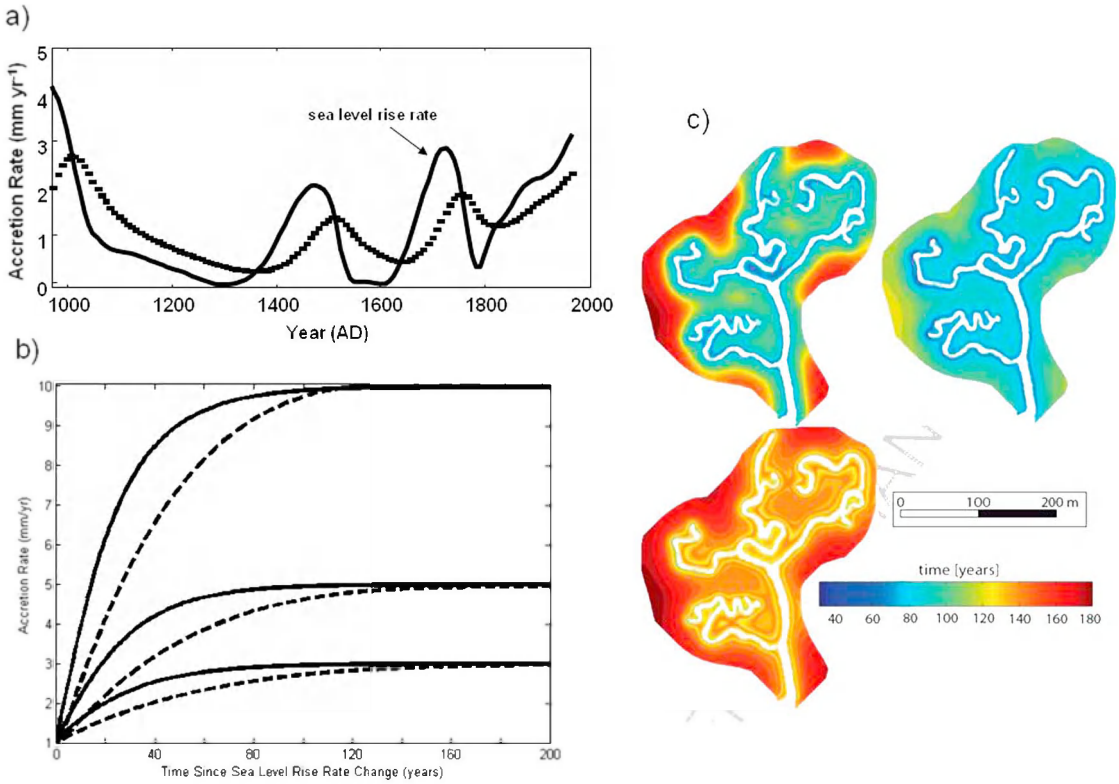

Figure 13. (a) Modeled response of marsh accretion rates to the last millennium of sea level change, simulated by the model of *Kirwan and Murray* [2007], demonstrating multidecadal lags between sea level change and marsh response. Sea level rise rates, denoted by the heavy solid line, are from *van de Plassche et al.* [1998]. Modified from *Kirwan and Murray* [2008a]. (b) Modeled accretion rates take on the order of 100 years to equilibrate to step changes in the rate of sea level rise. These experiments began with a marsh surface in equilibrium with a 1 mm yr^{-1} rate of sea level rise. Sea level rise rates increased abruptly to 3, 5, or 10 mm yr^{-1} at time zero. Black line, *Morris et al.* [2002] model; dashed line, *Temmerman et al.* [2003a, 2003b] model. Source: *Kirwan and Temmerman* [2009]. Copyright Elsevier 2009. (c) Comparison of local time lags between rates of marsh accretion and sea level rise for different sediment supply and sea level scenarios. The color scale represents the time intervals necessary for adjustment of different portions of the marsh. Clockwise from top: step change in the rate of SLR from R = 1 mm yr^{-1} to R = 3 mm yr^{-1}, $C0$ = 50 mg L^{-1}; step change in the rate of SLR from R = 3 mm yr^{-1} to R = 10 mm yr^{-1}, $C0$ = 50 mg L^{-1}; and step change in the rate of SLR from R = 1 mm yr^{-1} to R = 3 mm yr^{-1}, $C^*0 = C0/2$. Source: *D'Alpaos* [2011]. Copyright Elsevier 2009.

patterns of inundation for most of the 20th century and may just now be approaching a new equilibrium state. Alternatively, if recent increases in sea level rise rates are interpreted as a gradual acceleration, then properties of the marsh are always a few decades behind the physical conditions driving the change. In that case, observations of marsh adjustment such as transgression of plant zonation or expanding channel networks are underestimated, and more change should be expected even if rates of sea level rise were to stabilize [*Kirwan and Murray*, 2008a].

8.5. Threshold Sea Level Rise Rates for Marsh Survival

[94] While models of salt marsh evolution generally point to ecosystem resiliency, widespread observations of marsh submergence indicate that under some conditions, marshes simply cannot survive. In particular, marshes in estuaries with low tidal ranges and little mineral sediment appear to be vulnerable [*Reed*, 1995]. One limit to the survival of intertidal wetlands is the growth of vegetation itself. In the absence of vegetation, a number of ecogeomorphic processes (e.g., peat collapse, wave and channel erosion, and lack of accretion) lead to the rapid loss of elevation, precluding the return of vegetation [*DeLaune et al.*, 1994; *Fagherazzi et al.*, 2006; *Marani et al.*, 2007; *Kirwan et al.*, 2008]. Thus for a marsh to maintain its position in the intertidal zone, its elevation must never become so low that vegetation dies.

[95] *Kirwan et al.* [2010] summarized the conditions that lead to platform submergence in five numerical models and found that threshold rates of sea level rise for marsh survival vary by more than 2 orders of magnitude depending on an estuary's tidal range and sediment availability (Figure 14). At low tidal ranges and suspended sediment concentrations, marshes submerged at rates of sea level rise of only a few millimeters per year. However, under more favorable conditions,

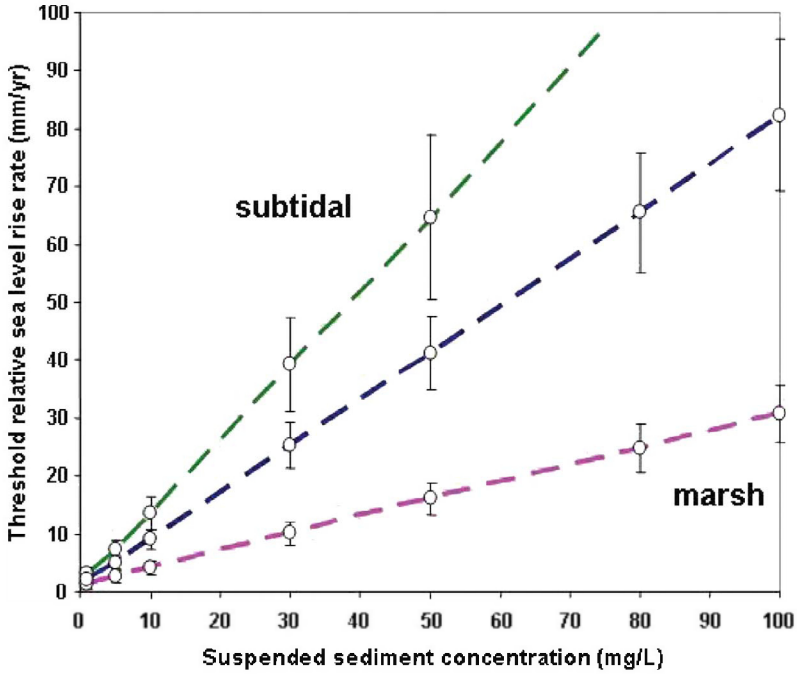

Figure 14. Predicted threshold rates of sea level rise, above which marshes are replaced by subtidal environments as the stable ecosystem. Each point (open circles) represents the mean threshold rate (±1 SE) predicted by five numerical models as a function of suspended sediment concentration and spring tidal range. Pink line denotes thresholds for marshes modeled under a 1 m tidal range, blue line denotes 3 m tidal range, and the green line denotes 5 m tidal range. Modified from *Kirwan et al.* [2010].

modeled marshes could survive several centimeters of sea level rise per year. Variation between models is surprisingly low given that they were designed to represent marshes from around the world (e.g., Venice Lagoon (Italy), North Inlet (South Carolina), and Scheldt Estuary (Belgium-Netherlands)) and consequently incorporate different dominant processes and approaches to modeling ecogeomorphic feedbacks (two treat organic accretion in detail while others treat mineral accretion in detail, and one does not model vegetation growth at all). Apparently, the coupling between inundation and accretion that is generally common to all models (k in equation (26)) leads to similar results regardless of the actual processes that are responsible for such a link or how they are modeled [*Kirwan and Temmerman*, 2009].

[96] Although wave erosion is not incorporated into these particular simulations, its effect is likely to enhance the threshold condition by introducing a positive feedback between inundation and erosion. In relatively shallow water, an increase in inundation leads to a decrease in bottom friction and therefore an increase in erosion rate and further platform lowering [*Fagherazzi et al.*, 2006]. Although vegetation growth can mitigate the feedback, when sea level rise lowers platform elevations so that vegetation cannot grow, waves quickly erode low intertidal surfaces into ones that are permanently inundated and incapable of regrowing vegetation [*Marani et al.*, 2007]. In fact, this process is likely responsible for the bimodal distribution of elevations in coastal lagoons where very few surfaces are at low intertidal elevations [*Fagherazzi et al.*, 2006].

8.6. Predictions for the Future

[97] The threshold rates of sea level rise identified in the previous section (Figure 14) offer insight into how coastal wetlands will respond to future sea level rise. As a first approximation, the fate of any particular marsh can be evaluated simply by knowing the suspended sediment concentration and tidal range of the estuary. Using the Plum Island Estuary, Massachusetts, United States, as an example (SSC = 1 mg L^{-1} and TR = 3 m), the model ensemble predicts a threshold rate of sea level rise of 4 mm yr^{-1}. While stable at historical rates of relative sea level rise (~3 mm yr^{-1} locally), even a slight acceleration would push marshes in this estuary into the unstable portion of the graph. On the other hand, with high sediment availability (e.g., Yantze River Delta, China; SSC = 1000 mg L^{-1} and TR ~ 5 m), the modeling framework predicts marshes to be stable at virtually any realistic sea level rise rate. *Kirwan et al.* [2010] conclude that while a moderate IPCC style acceleration in the rate of sea level rise would threaten marshes in a few estuaries, most would remain stable. However, faster accelerations in the rate of sea level rise (>1 m by 2100 [*Rahmstorf*, 2007]) would submerge all but the most sediment rich marshes [*Kirwan et al.*, 2010].

[98] Although point-based models of vertical elevation change converge to fairly similar results (Figures 14 and 15a), there is considerably less confidence in how elevation trajectories will vary spatially, particularly where influenced by waves and vegetation zonation. High marshes are subject to different processes than low marshes (e.g., the role of organic accumulation increases with elevation), and vegetation

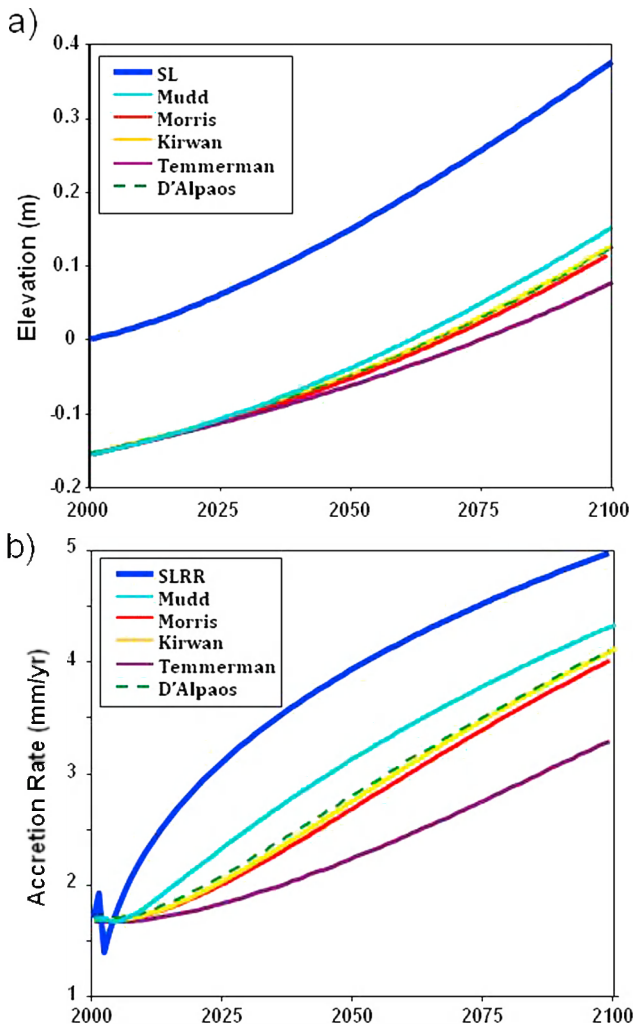

Figure 15. Response of (a) marsh elevation and (b) accretion rate to a conservative sea level acceleration (IPCC A1B scenario [*Bindoff et al.*, 2007]) as predicted by five point models of salt marsh evolution. The heavy blue line denotes sea level at spring high water (Figure 15a) or the sea level rise rate (Figure 15b). Since sea level rise rates tend to exceed accretion rates, marsh elevations adjust to sea level acceleration by becoming lower relative to sea level (i.e., more inundated) (Figure 15a), which enhanced vertical accretion (Figure 15b). (Experimental conditions: spring tidal range = 1 m, suspended sediment concentration = 30 mg L^{-1}) [from *Kirwan et al.*, 2010].

species with different tolerance to flooding interact in ways that can enable or inhibit survival of neighboring species [*Morris*, 2006]. Moreover, point-based models miss potentially important interactions between different portions of the marsh system. For example, channel erosion that accompanies platform deepening may bring extra sediment to interior portions of the marsh platform [*D'Alpaos et al.*, 2007a; *Kirwan et al.*, 2008]. Alternatively, gradual platform submergence may be accelerated by the positive feedback between inundation and wave erosion [*Fagherazzi et al.*, 2006; *Marani et al.*, 2007]. Incorporating these types of complexities, common in real intertidal systems, remains an important goal for the next generation of salt marsh models.

[99] Existing spatially explicit models help solve some of these problems. Large-scale, landscape-style models consider separately the evolution of different vegetation types, and some treat organic accumulation in detail [e.g., *Reyes et al.*, 2000; *Craft et al.*, 2009; *Kairis and Rybczyk*, 2010]. These models document the transgression of vegetation zones and demonstrate that loss of a particular type of marsh occurs well before the complete drowning of all marshland [*Craft et al.*, 2009; *Reyes et al.*, 2000; *Kirwan and Murray*, 2008b; *Kairis and Rybczyk*, 2010] (Figure 11). Although salt marsh edge erosion is not comprehensively treated [e.g., *Mariotti and Fagherazzi*, 2010], landscape models offer insight into the potential expansion of marshes in the upslope direction. Simulations on the Georgia Coast, for example, suggest that brackish marshes and shrub-marsh transition areas will expand [*Craft et al.*, 2009]. Similarly, simulations on the Fraser River Delta, Canada, predict that, in the absence of dykes, marsh expansion would more than account for loss of salt marsh due to sea level rise over the next century [*Kirwan and Murray*, 2008b]. Nevertheless, treatments of processes in these landscape-scale models are necessarily simplistic and in some cases may overestimate predicted change [*Kirwan and Guntenspergen*, 2009]. More detailed, process-based models consider important interactions between the channel network and marsh platform, between wave erosion and vertical accretion, and the competition between marsh erosion at the seaward edge and marsh expansion at the landward edge. However, at present, these tend to be most suitable for exploring the general evolution of a schematic wetland or simulating a very specific location.

9. CONCLUSIONS

[100] The first generation of models of salt marsh evolution simulated deposition and accretion processes only along the vertical dimension (point models [see *Allen*, 1994; *Woolnough et al.*, 1995]). These models are simple and of great conceptual value, but fail to represent the richness of the marsh landscape. In recent years, several researchers introduced the spatial distribution of sediment fluxes and vegetation characteristics in their modeling frameworks. Existing spatial models range, with increasing complexity, from simple empirical models that predict sedimentation patterns as a function of topographic variables [*Temmerman et al.*, 2003a] to physically based models that simulate water and sediment flow paths on the basis of simplified hydrodynamic schemes [*D'Alpaos et al.*, 2007a; *Rinaldo et al.*, 1999b] or on the basis of a full hydrodynamic description of the feedbacks between tidal flow and vegetation [*Temmerman et al.*, 2005b]. All of these approaches have their potentials and limitations. For example, the numerically simpler models allow the computation of long-term morphological changes as the result of platform sediment fluxes and the interaction with other eco-geomorphological units of tidal marshes, such as the channel dynamics [*D'Alpaos et al.*, 2007a]. Complex hydrodynamic modeling provides an opportunity to gain fundamental

insights in sediment flux mechanisms, such as the role of vegetation-flow interactions [*Temmerman et al.*, 2005b].

[101] A key component of numerical models of salt marsh evolution is the coupling between geomorphology and ecology. This coupling must be quantitative, i.e., described by process-based equations that can be included in numerical codes. Moreover, the parameters of these equations should be derived by field or laboratory experiments. In sections 5 and 6 we presented a brief overview of the parametric equations currently used in salt marsh models, but these studies are still in their infancy, and more research is clearly needed to address the influence of biota on morphology and sediment transport. In fact, several of the expressions used in current models were derived for specific geographical locations, and their inclusion in global models is of doubtful validity. The first interdisciplinary studies involving engineers, biologists, and geologists have started to address these important feedbacks, providing the basic blocks for the next generation of marsh models [see, e.g., *Mudd et al.*, 2009; *Kirwan et al.*, 2009; *Fagherazzi et al.*, 2011].

[102] Sediment transport dynamics in current models of salt marsh evolution are extremely simplified and are only a starting point for the representation of these systems. More refined models will need to account for complex erosive and depositional processes in cohesive sediments, the effect of biota on sediment transport processes, the sedimentology of organic matter, and the effect of grain size distribution on erosion and deposition.

[103] Most of the models presented in this review describe the morphological evolution of salt marshes as a continuous process regulated by slowly varying inputs of sediment and sea level rise. In reality both erosion and deposition are stochastic in nature, with infrequent events like storms, hurricanes, and heavy rainfalls producing most of the geomorphic work. Storms trigger wave attack of marsh boundaries and removal of the vegetation mat [*Priestas and Fagherazzi*, 2011], as well as enhance sediment remobilization in the subtidal area leading to high transport and deposition on the marsh surface [*Mariotti and Fagherazzi*, 2010]. The inclusion of the variability of external drivers in salt marsh models is still in a primordial phase [see, e.g., *Rybczyk and Cahoon*, 2002], and more research is clearly needed on this important topic.

[104] A few conclusions arise from the applications of marsh models to climate change and the dynamics of sea level rise. First, the point-based vertical evolution models clearly indicate that large swaths of marshland will persist under conservative projections of sea level rise during the next century, but will submerge under faster scenarios. In either case, sea level change will be accompanied by a lowering of platform elevations that will lead to a migration of vegetation zones, and landscape models predict the loss of some vegetation types. More detailed geomorphic models predict that platform lowering will be accompanied by an expansion of the channel network, wave scour, and lateral erosion of the marsh edge. However, these models are for now unable to discern between a few basic outcomes. For example, the models presented herein cannot determine whether upland expansion of marshes can compensate for erosion of the salt marsh edge and vertical submergence of the platform. They cannot quantify the relative importance of the sediment delivery to the marsh interior from an expanding channel network or the positive feedback between wave erosion and inundation.

[105] Further studies are also needed for uncertainty quantification and error estimation of the model results. In fact, several of the numerical frameworks presented herein are based on simplified assumptions, on sparse data sets very often site-specific, and on parameters that might display high variability in nature.

[106] **ACKNOWLEDGMENTS.** S.F. was supported by the National Science Foundation, LENS project awards OCE 0924287 and OCE 0923689, the VCR-LTER program award DEB 0621014, and by the Office of Naval Research award N00014-10-1-0269. G.R.G. and M.L.K. gratefully acknowledge support from the U.S. Geological Survey Global Change Research Program.

[107] Greg Okin thanks two technical reviewers and one cross-disciplinary reviewer.

REFERENCES

Allen, J. R. L. (1989), Evolution of salt marsh cliffs in muddy and sandy systems: A qualitative comparison of British west-coast estuaries, *Earth Surf. Processes Landforms*, *14*, 85–92, doi:10.1002/esp.3290140108.

Allen, J. R. L. (1994), A continuity-based sedimentological model for temperate-zone tidal salt marshes, *J. Geol. Soc.*, *151*, 41–49, doi:10.1144/gsjgs.151.1.0041.

Allen, J. R. L. (1995), Salt marsh growth and fluctuating sea level: Implications of a simulation model for Flandrian coastal stratigraphy and peat-based sea-level curves, *Sediment. Geol.*, *100*, 21–45, doi:10.1016/0037-0738(95)00101-8.

Allen, J. R. L. (2000), Morphodynamics of Holocene salt marshes: A review sketch from the Atlantic and southern North Sea Coasts of Europe, *Quat. Sci. Rev.*, *19*, 1155–1231, doi:10.1016/S0277-3791(99)00034-7.

Allen, J. R. L., and K. Pye (1992), *Saltmarshes: Morphodynamics, Conservation, and Engineering Significance*, 196 pp., Cambridge Univ. Press, U. K.

Beeftink, W. G. (1966), Vegetation and habitat of the salt marshes and beach plains in the south-western part of the Netherlands, *Wentia*, *15*, 83–108.

Bindoff, N. L., et al. (2007), Observations: Oceanic climate change and sea level, in Climate Change 2007: The Physical Science Basis. Contribution of Working Group I to the Fourth Assessment Report of the Intergovernmental Panel on Climate Change, edited by S. Solomon et al., pp. 385–432, Cambridge Univ. Press, Cambridge, U. K.

Blum, L. K. (1993), *Spartina alterniflora* root dynamics in a Virginia marsh, *Mar. Ecol. Prog. Ser.*, *102*, 169–178, doi:10.3354/meps102169.

Boon, J. D., III (1975), Tidal discharge asymmetry in a salt marsh drainage system, *Limnol. Oceanogr.*, *20*, 71–80, doi:10.4319/lo.1975.20.1.0071.

Bouma, T. J., M. B. De Vries, E. Low, L. Kusters, P. M. J. Herman, I. C. Tanczos, A. Hesselink, S. Temmerman, P. Meire, and S. Van Regenmortel (2005a), Hydrodynamic measurements on a mudflat and in salt marsh vegetation: Identifying general relationships for habitat characterisations, *Hydrobiologia*, *540*, 259–274, doi:10.1007/s10750-004-7149-0.

Bouma, T. J., M. B. De Vries, E. Low, G. Peralta, I. Tanczos, J. Van de Koppel, and P. M. J. Herman (2005b), Trade-offs related to ecosystem-engineering: A case study on stiffness of

emerging macrophytes, *Ecology*, *86*(8), 2187–2199, doi:10.1890/04-1588.

Bouma, T. J., L. A. van Duren, S. Temmerman, T. Claverie, A. Blanco-Garcia, T. Ysebaert, and P. M. J. Herman (2007), Spatial flow and sedimentation patterns within patches of epibenthic structures: Combining field, flume, and modelling experiments, *Cont. Shelf Res.*, *27*(8), 1020–1045, doi:10.1016/j.csr.2005.12.019.

Bouma, T. J., M. Friedrichs, P. Klaassen, B. K. van Wesenbeeck, F. G. Brun, S. Temmerman, M. M. van Katwijk, G. Graf, and P. M. J. Herman (2009), Effects of shoot stiffness, shoot size, and current velocity on scouring sediment from around seedlings and propagules, *Mar. Ecol. Prog. Ser.*, *388*, 293–297, doi:10.3354/meps08130.

Bricker-Urso, S., S. W. Nixon, J. K. Cochran, D. J. Hirschberg, and C. Hunt (1989), Accretion rates and sediment accumulation in Rhode Island salt marshes, *Estuaries*, *12*(4), 300–317, doi:10.2307/1351908.

Cahoon, D. R., and D. J. Reed (1995), Relationships among marsh surface topography, hydroperiod, and soil accretion in a deteriorating Louisiana salt marsh, *J. Coastal Res.*, *11*, 357–369.

Cahoon, D. R., et al. (2003), Mass tree mortality leads to mangrove peat collapse at Bay Islands, Honduras after Hurricane Mitch, *J. Ecol.*, *91*(6), 1093–1105.

Cahoon, D. R., P. F. Hensel, T. Spencer, D. J. Reed, K. L. McKee, and N. Saintilan (2006), Coastal wetland vulnerability to relative sea-level rise: Wetland elevation trends and process controls, in *Wetlands and Natural Resource Management*, *Ecol. Stud.*, vol. 190, edited by J. T. A. Verhoeven et al., pp. 271–292, Springer, New York.

Callaway, J. C., R. D. DeLaune, and W. H. Patrick (1997), Sediment accretion rates from four coastal wetlands along the Gulf of Mexico, *J. Coastal Res.*, *13*(1), 181–191.

Chmura, G. L., S. C. Anisfeld, D. R. Cahoon, and J. C. Lynch (2003), Global carbon sequestration in tidal, saline wetland soils, *Global Biogeochem. Cycles*, *17*(4), 1111, doi:10.1029/2002GB001917.

Christiansen, T., P. L. Wiberg, and T. G. Milligan (2000), Flow and sediment transport on a tidal salt marsh surface, *Estuarine Coastal Shelf Sci.*, *50*(3), 315–331, doi:10.1006/ecss.2000.0548.

Church, J. A., and N. J. White (2006), A 20th century acceleration in global sea-level rise, *Geophys. Res. Lett.*, *33*, L01602, doi:10.1029/2005GL024826.

Church, J. A., et al. (2001), Changes in sea level, in *Climate Change 2001: The Scientific Basis. Contribution of Working Group I to the Third Assessment Report of the Intergovernmental Panel on Climate Change*, edited by J. T. Houghton et al., pp. 639–694, Cambridge Univ. Press, Cambridge, U. K.

Collins, L. M., J. N. Collins, and L. B. Leopold (1987), Geomorphic processes of an estuarine marsh: Preliminary results and hypotheses, in *International Geomorphology 1986*, edited by V. Gardner, pp. 1049–1072, John Wiley, Hoboken, N. J.

Conn, C. E., and F. P. Day (1997), Root decomposition across a barrier island chronosequence: Litter quality and environmental controls, *Plant Soil*, *195*(2), 351–364, doi:10.1023/A:1004214216889.

Costanza, R., and M. Ruth (1998), Using dynamic systems modeling to scope environmental problems and build consensus, *Environ. Manage. N. Y.*, *22*, 183–195, doi:10.1007/s002679900095.

Costanza, R., and A. Voinov (2004), *Landscape Simulation Modeling: A Spatially Explicit, Dynamic Approach*, 330 pp., Springer, New York.

Costanza, R., F. H. Sklar, and M. L. White (1990), Modeling coastal landscape dynamics, *BioScience*, *40*(2), 91–107, doi:10.2307/1311342.

Craft, C., J. Clough, J. Ehman, S. Joye, D. Park, S. Pennings, H. Guo, and M. Machmuller (2009), Forecasting the effects of accelerated sea level rise on tidal marsh ecosystem services, *Frontiers Ecol. Environ*, *7*, 73–78, doi:10.1890/070219.

D'Alpaos, A. (2011), The mutual influence of biotic and abiotic components on the long-term ecomorphodynamic evolution of salt marsh ecosystems, *Geomorphology*, *126*(3–4), 269–278.

D'Alpaos, A., S. Lanzoni, M. Marani, S. Fagherazzi, and A. Rinaldo (2005), Tidal network ontogeny: Channel initiation and early development, *J. Geophys. Res.*, *110*, F02001, doi:10.1029/2004JF000182.

D'Alpaos, A., S. Lanzoni, S. M. Mudd, and S. Fagherazzi (2006), Modeling the influence of hydroperiod and vegetation on the cross-sectional formation of tidal channels, *Estuarine Coastal Shelf Sci.*, *69*(3–4), 311–324, doi:10.1016/j.ecss.2006.05.002.

D'Alpaos, A., S. Lanzoni, M. Marani, and A. Rinaldo (2007a), Landscape evolution in tidal embayments: Modeling the interplay of erosion sedimentation and vegetation dynamics, *J. Geophys. Res.*, *112*, F01008, doi:10.1029/2006JF000537.

D'Alpaos, A., S. Lanzoni, M. Marani, A. Bonometto, G. Cecconi, and A. Rinaldo (2007b), Spontaneous tidal network formation within a constructed salt marsh: Observations and morphodynamic modelling, *Geomorphology*, *91*(3–4), 186–197, doi:10.1016/j.geomorph.2007.04.013.

D'Alpaos, A., S. Lanzoni, A. Rinaldo, and M. Marani (2009), Intertidal eco-geomorphological dynamics and hydrodynamic circulation, in *Coastal Wetlands: An Integrated Ecosystem Approach*, edited by G. M. E. Perillo et al., pp. 159–179, Elsevier, Amsterdam.

Darby, F. A., and R. E. Turner (2008a), Effects of eutrophication on salt marsh root and rhizome biomass accumulation, *Mar. Ecol. Prog. Ser.*, *363*, 63–70, doi:10.3354/meps07423.

Darby, F. A., and R. E. Turner (2008b), Below- and aboveground *Spartina alterniflora* production in a Louisiana salt marsh, *Estuaries Coasts*, *31*(1), 223–231, doi:10.1007/s12237-007-9014-7.

Davidson-Arnott, R. G. D., D. Van Proosdij, J. Ollerhead, and L. Schostak (2002), Hydrodynamics and sedimentation in salt marshes: Examples from a macrotidal marsh, Bay of Fundy, *Geomorphology*, *48*(1–3) 209–231, doi:10.1016/S0169-555X(02)00182-4.

Day, J. W., J. Rybczyk, F. Scarton, A. Rismondo, D. Are, and G. Cecconi (1999), Soil accretionary dynamics, sea-level rise and the survival of wetlands in Venice Lagoon: A field and modeling approach, *Estuarine Coastal Shelf Sci.*, *49*, 607–628, doi:10.1006/ecss.1999.0522.

Day, J. W., et al. (2005), Implications of global climatic change and energy cost and availability for the restoration of the Mississippi Delta, *Ecol. Eng.*, *24*(4), 253–265, doi:10.1016/j.ecoleng.2004.11.015.

DeLaune, R. D., J. A. Nyman, and W. H. Patrick (1994), Peat collapse, ponding, and wetland loss in a rapidly submerging coastal marsh, *J. Coastal Res.*, *10*, 1021–1030.

Donnelly, J. P., and M. D. Bertness (2001), Rapid shoreward encroachment of salt marsh cordgrass in response to accelerated sea-level rise, *Proc. Natl. Acad. Sci. U. S. A.*, *98*, 14,218–14,223, doi:10.1073/pnas.251209298.

Donnelly, J. P., P. Cleary, P. Newby, and R. Ettinger (2004), Coupling instrumental and geological records of sea-level change: Evidence from southern New England of an increase in the rate of sea-level rise in the late 19th century, *Geophys. Res. Lett.*, *31*, L05203, doi:10.1029/2003GL018933.

Fagherazzi, S., and D. J. Furbish (2001), On the shape and widening of salt marsh creeks, *J. Geophys. Res.*, *106*(C1), 991–1003, doi:10.1029/1999JC000115.

Fagherazzi, S., and T. Sun (2004), A stochastic model for the formation of channel networks in tidal marshes, *Geophys. Res. Lett.*, *31*, L21503, doi:10.1029/2004GL020965.

Fagherazzi, S., and P. L. Wiberg (2009), Importance of wind conditions, fetch, and water levels on wave-generated shear stresses in shallow intertidal basins, *J. Geophys. Res.*, *114*, F03022, doi:10.1029/2008JF001139.

Fagherazzi, S., A. Bortoluzzi, W. E. Dietrich, A. Adami, M. Marani, S. Lanzoni, and A. Rinaldo (1999), Tidal networks: 1. Automatic

network extraction and preliminary scaling features from digital terrain maps, *Water Resour. Res.*, *35*(12), 3891–3904, doi:10.1029/1999WR900236.

Fagherazzi S., P. L. Wiberg, and A. D. Howard (2003) Tidal flow field in a small basin, *J. Geophys. Res.*, *108*(C3), 3071, doi:10.1029/2002JC001340.

Fagherazzi, S., M. Marani, and L. K. Blum (2004a), Introduction: The coupled evolution of geomorphological and ecosystem structures in salt marshes, in *The Ecogeomorphology of Tidal Marshes*, *Coastal Estuarine Stud.*, vol. 59, edited by S. Fagherazzi, M. Marani, and L. K. Blum, pp. 1–5, AGU, Washington, D. C.

Fagherazzi, S., E. J. Gabet, and D. J. Furbish (2004b), The effect of bidirectional flow on tidal channel planforms, *Earth Surf. Processes Landforms*, *29*(3), 295–309, doi:10.1002/esp.1016.

Fagherazzi, S., L. Carniello, L. D'Alpaos, and A. Defina (2006), Critical bifurcation of shallow microtidal landforms in tidal flats and salt marshes, *Proc. Natl. Acad. Sci. U. S. A.*, *103*(22), 8337–8341, doi:10.1073/pnas.0508379103.

Fagherazzi, S., M. Hannion, and P. D'Odorico (2008), Geomorphic structure of tidal hydrodynamics in salt marsh creeks, *Water Resour. Res.*, *44*(2), W02419, doi:10.1029/2007WR006289.

Fagherazzi, S., D. M. FitzGerald, R. W. Fulweiler, Z. Hughes, P. L. Wiberg, K. J. McGlathery, J. T. Morris, T. J. Tolhurst, L. A. Deegan, and D. S. Johnson (2011), Ecogeomorphology of salt marshes, in *Treatise on Geomorphology*, vol. 12, *Ecogeomorphology*, edited by D. Butler and C. Hupp, Elsevier, New York, in press.

Feagin, R. A., S. M. Lozada-Bernard, T. M. Ravens, I. Moeller, K. M. Yeager, and A. H. Baird (2009), Does vegetation prevent wave erosion of salt marsh edges?, *Proc. Natl. Acad. Sci. U. S. A.*, *106*(25), 10,109–10,113.

Feola, A., E. Belluco, A. D'Alpaos, S. Lanzoni, M. Marani, and A. Rinaldo (2005), A geomorphic study of lagoonal landforms, *Water Resour. Res.*, *41*, W06019, doi:10.1029/2004WR003811.

Fragoso, G., and T. Spencer (2008), Physiographic control on the development of *Spartina* marshes, *Science*, *322*(5904), 1064.

Fitz, H. C., E. B. DeBellevue, R. Costanza, R. Boumans, T. Maxwell, L. Wainger, and F. H. Sklar (1996), Development of a general ecosystem model for a range of scales and ecosystems, *Ecol. Modell.*, *88*, 263–295, doi:10.1016/0304-3800(95)00112-3.

French, J. R. (1993), Numerical simulation of vertical marsh growth and adjustment to accelerated sea-level rise, North Norfolk, UK, *Earth Surf. Processes Landforms*, *18*, 63–81, doi:10.1002/esp.3290180105.

French, J. (2006), Tidal marsh sedimentation and resilience to environmental change: Exploratory modeling of tidal, sea-level, and sediment supply forcing in predominantly allochthonous systems, *Mar. Geol.*, *235*, 119–136, doi:10.1016/j.margeo.2006.10.009.

French, J. R., and D. R. Stoddart (1992), Hydrodynamics of salt marsh creek systems: Implications for marsh morphological development and material exchange, *Earth Surf. Processes Landforms*, *17*(3), 235–252, doi:10.1002/esp.3290170304.

French, J. R., T. Spencer, A. L. Murray, and N. S. Arnold (1995), Geostatistical analysis of sediment deposition in two small tidal wetlands, Norfolk, United Kingdom, *J. Coastal Res.*, *11*, 308–321.

Friedrichs, C. T., and J. E. Perry (2001), Tidal salt marsh morphodynamics, *J. Coastal Res.*, *27*, 6–36.

Gabet, E. (1998), Lateral migration and bank erosion in a salt marsh tidal channel in San Francisco Bay, California, *Estuaries*, *21*(4), 745–753, doi:10.2307/1353278.

Gardner, D., and M. Bohn (1980), Geomorphic and hydraulic evolution of tidal creeks on a subsiding beach ridge plain, North Inlet, S.C., *Mar. Geol.*, *34*, M91–M97, doi:10.1016/0025-3227(80)90067-5.

Garofalo, D. (1980), The influence of wetland vegetation on tidal stream migration and morphology, *Estuaries*, *3*(4), 258–270, doi:10.2307/1352081.

Gedan, K. B., M. L. Kirwan, E. Wolanski, E. B. Barbier, and B. R. Silliman (2011), The present and future role of coastal wetland vegetation in protecting shorelines: Answering recent challenges to the paradigm, *Clim. Change*, *106*, 7–29, doi:10.1007/s10584-010-0003-7.

Gehrels, W. R., B. W. Hayward, R. M. Newnham, and K. E. Southall (2008), A 20th century acceleration of sea-level rise in New Zealand, *Geophys. Res. Lett.*, *35*, L02717, doi:10.1029/2007GL032632.

Gleason, M. L., D. A. Elmer, N. C. Pien, and J. S. Fisher (1979), Effects of stem density upon sediment retention by salt marsh cord grass, *Spartina alterniflora* Loisel, *Estuaries*, *2*(4), 271–273, doi:10.2307/1351574.

Gutierrez, M., and M. Wangen (2005), Modeling of compaction and overpressuring in sedimentary basins, *Mar. Pet. Geol.*, *22*(3), 351–363, doi:10.1016/j.marpetgeo.2005.01.003.

Hack, J. T. (1957), Studies of longitudinal profiles in Virginia and Maryland, *U.S. Geol. Surv. Prof. Pap.*, *294-B*, 45–97.

Hartig, E. K., V. Gornitz, A. Kolker, F. Mushacke, and D. Fallon (2002), Anthropogenic and climate-change impacts on salt marshes of Jamaica Bay, New York City, *Wetlands*, *22*, 71–89, doi:10.1672/0277-5212(2002)022[0071:AACCIO]2.0.CO;2.

Hood, W. G. (2006), A conceptual model of depositional, rather than erosional, tidal channel development in the rapidly prograding Skagit River Delta (Washington, USA), *Earth Surf. Processes Landforms*, *31*(14), 1824–1838, doi:10.1002/esp.1381.

Howes, N. C., D. M. Fitzgerald, Z. J. Hughes, I. Y. Georgiou, M. A. Kulp, M. D. Miner, J. M. Smith, and J. A. Barras (2010), Hurricane-induced failure of low salinity wetlands, *Proc. Natl. Acad. Sci. U. S. A.*, *107*, 14,014–14,019, doi:10.1073/pnas.0914582107.

Hughes, Z. J., D. M. FitzGerald, C. A. Wilson, S. C. Pennings, K. Wieski, and A. Mahadevan (2009), Rapid headward erosion of marsh creeks in response to relative sea level rise, *Geophys. Res. Lett.*, *36*, L03602, doi:10.1029/2008GL036000.

Jevrejeva, S., J. C. Moore, A. Grinsted, and P. L. Woodworth (2008), Recent global sea level acceleration started over 200 years ago?, *Geophys. Res. Lett.*, *35*, L08715, doi:10.1029/2008GL033611.

Kairis, P., and J. M. Rybczyk (2010), A spatially explicit relative elevation model for Padilla Bay, WA, *Ecol. Modell.*, *221*(7), 1005–1016, doi:10.1016/j.ecolmodel.2009.01.025.

Kearney, M. S., R. E. Grace, and J. C. Stevenson (1988), Marsh loss in the Nanticoke Estuary, Chesapeake Bay, *Geogr. Rev.*, *78*, 205–220, doi:10.2307/214178.

Kearney, M. S., A. S. Rogers, J. R. G. Townshend, E. Rizzo, D. Stutzer, J. C. Stevenson, and K. Sundborg (2002), Landsat imagery shows decline of coastal marshes in Chesapeake and Delaware Bays, *Eos Trans. AGU*, *83*(16), 173–178, doi:10.1029/2002EO000112.

Kim, S. C., C. T. Friedrichs, J. P. Y. Maa, and L. D. Wright (2000), Estimating bottom stress in tidal boundary layer from Acoustic Doppler Velocimeter data, *J. Hydraul. Eng.*, *126*(6), 399–406, doi:10.1061/(ASCE)0733-9429(2000)126:6(399).

Kirwan, M. L., and G. R. Guntenspergen (2009), Accelerated sea-level rise: A response to Craft et al., *Frontiers Ecol. Environ*, *7*, 126–127, doi:10.1890/09.WB.005.

Kirwan, M. L., and G. R. Guntenspergen (2010), The influence of tidal range on the stability of coastal marshland, *J. Geophys. Res.*, *115*, F02009, doi:10.1029/2009JF001400.

Kirwan, M. L., and A. Murray (2007), A coupled geomorphic and ecological model of tidal marsh evolution, *Proc. Natl. Acad. Sci. U. S. A.*, *104*(15), 6118–6122, doi:10.1073/pnas.0700958104.

Kirwan, M. L., and A. B. Murray (2008a), Tidal marshes as disequilibrium landscapes? Lags between morphology and Holocene sea level change, *Geophys. Res. Lett.*, *35*, L24401, doi:10.1029/2008GL036050.

Kirwan, M. L., and A. B. Murray (2008b), Ecological and morphological response of brackish tidal marshland to the next century of

sea level rise: Westham Island, British Columbia, *Global Planet. Change*, *60*, 471–486, doi:10.1016/j.gloplacha.2007.05.005.

Kirwan, M. L., and S. Temmerman (2009), Coastal marsh response to historical and future sea-level acceleration, *Quat. Sci. Rev.*, *28*, 1801–1808, doi:10.1016/j.quascirev.2009.02.022.

Kirwan, M. L., A. Murray, and W. Boyd (2008), Temporary vegetation disturbance as an explanation for permanent loss of tidal wetlands, *Geophys. Res. Lett.*, *35*, L05403, doi:10.1029/2007GL032681.

Kirwan, M. L., G. R. Guntenspergen, and J. T. Morris (2009), Latitudinal trends in *Spartina alterniflora* productivity and the response of coastal marshes to global change, *Global Change Biol.*, *15*(8), 1982–1989, doi:10.1111/j.1365-2486.2008.01834.x.

Kirwan, M. L., G. R. Guntenspergen, A. D'Alpaos, J. T. Morris, S. M. Mudd, and S. Temmerman (2010), Limits on the adaptability of coastal marshes to rising sea level, *Geophys. Res. Lett.*, *37*, L23401, doi:10.1029/2010GL045489.

Langley, J. A., K. L. Mckee, D. R. Cahoon, J. A. Cherry, and J. P. Megonigal (2009), Elevated CO_2 stimulates marsh elevation gain, counterbalancing sea-level rise, *Proc. Natl. Acad. Sci. U. S. A.*, *106*(15), 6182–6186.

Le Hir, P., Y. Monbet, and F. Orvain (2007), Sediment erodability in sediment transport modeling: Can we account for biota effects?, *Cont. Shelf Res.*, *27*, 1116–1142, doi:10.1016/j.csr.2005.11.016.

Leonard, L. A. (1997), Controls on sediment transport and deposition in an incised mainland marsh basin, southeastern North Carolina, *Wetlands*, *17*, 263–274, doi:10.1007/BF03161414.

Leonard, L. A., and A. L. Croft (2006), The effect of standing biomass on flow velocity and turbulence in *Spartina alterniflora* canopies, *Estuarine Coastal Shelf Sci.*, *69*(3–4), 325–336, doi:10.1016/j.ecss.2006.05.004.

Leonard, L. A., and M. E. Luther (1995), Flow hydrodynamics in tidal marsh canopies, *Limnol. Oceanogr.*, *40*(8), 1474–1484, doi:10.4319/lo.1995.40.8.1474.

Li, H., and S. L. Yang (2009), Trapping effect of tidal marsh vegetation on suspended sediment, Yangtze Delta, *J. Coastal Res.*, *25*(4), 915–936, doi:10.2112/08-1010.1.

Lightbody, A. F., and H. M. Nepf (2006), Prediction of velocity profiles and longitudinal dispersion in emergent salt marsh vegetation, *Limnol. Oceanogr.*, *51*, 218–228, doi:10.4319/lo.2006.51.1.0218.

Marani, M., S. Lanzoni, D. Zandolin, G. Seminara, and A. Rinaldo (2002), Tidal meanders, *Water Resour. Res.*, *38*(11), 1225, doi:10.1029/2001WR000404.

Marani, M., S. Lanzoni, E. Belluco, A. D'Alpaos, A. Defina, and A. Rinaldo (2003), On the drainage density of tidal networks, *Water Resour. Res.*, *39*(2), 1040, doi:10.1029/2001WR001051.

Marani, M., S. Lanzoni, S. Silvestri, and A. Rinaldo (2004), A Tidal landforms, patterns of halophytic vegetation and the fate of the lagoon of Venice, *J. Mar. Syst.*, *51*(1–4), 191–210, doi:10.1016/j.jmarsys.2004.05.012.

Marani, M., E. Belluco, S. Ferrari, S. Silvestri, A. D'Alpaos, S. Lanzoni, A. Feola, and A. Rinaldo (2006), Analysis, synthesis and modelling of high-resolution observations of salt marsh eco-geomorphological patterns in the Venice lagoon, *Estuarine Coastal Shelf Sci.*, *69*(3–4), 414–426, doi:10.1016/j.ecss.2006.05.021.

Marani, M., A. D'Alpaos, S. Lanzoni, L. Carniello, and A. Rinaldo (2007), Biologically controlled multiple equilibria of tidal landforms and the fate of the Venice lagoon, *Geophys. Res. Lett.*, *34*, L11402, doi:10.1029/2007GL030178.

Marani, M., A. D'Alpaos, S. Lanzoni, L. Carniello, and A. Rinaldo (2010), The importance of being coupled: Stable states and catastrophic shifts in tidal biomorphodynamics, *J. Geophys. Res.*, *115*, F04004, doi:10.1029/2009JF001600.

Marciano, R., Z. B. Wang, A. Hibma, H. J. de Vriend, and A. Defina (2005), Modeling of channel patterns in short tidal basins, *J. Geophys. Res.*, F01001, doi:10.1029/2003JF000092.

Marion, C., E. J. Anthony, and A. Trentesaux (2009), Short-term (<= 2 yrs) estuarine mudflat and saltmarsh sedimentation: High-resolution data from ultrasonic altimetery, rod surface-elevation table, and filter traps, *Estuarine Coastal Shelf Sci.*, *83*, 475–484, doi:10.1016/j.ecss.2009.03.039.

Mariotti, G., and S. Fagherazzi (2010), A numerical model for the coupled long-term evolution of salt marshes and tidal flats, *J. Geophys. Res.*, *115*, F01004, doi:10.1029/2009JF001326.

Mariotti, G., S. Fagherazzi, P. L. Wiberg, K. J. McGlathery, L. Carniello, and A. Defina (2010), Influence of storm surges and sea level on shallow tidal basin erosive processes, *J. Geophys. Res.*, *115*, C11012, doi:10.1029/2009JC005892.

Martin, J. F., E. Reyes, G. P. Kemp, H. Mashriqui, and J. W. Day (2002), Landscape modeling of the Mississippi Delta, *BioScience*, *52*(4), 357–365, doi:10.1641/0006-3568(2002)052[0357:LMOTMD]2.0.CO;2.

McKee, K. L., and W. H. Patrick (1988), The relationship of smooth cordgrass (*Spartina alterniflora*) to tidal datums: A review, *Estuaries*, *11*(3), 143–151, doi:10.2307/1351966.

Mcleod, E., B. Poulter, J. Hinkel, E. Reyes, and R. Salm (2010), Sea-level rise impact models and environmental conservation: A review of models and their applications, *Ocean Coast. Manage.*, *53*, 507–517, doi:10.1016/j.ocecoaman.2010.06.009.

Mesri, G., T. D. Stark, M. A. Ajlouni, and C. S. Chen (1997), Secondary compression of peat with or without surcharging, *J. Geotech. Geoenviron. Eng.*, *123*(5), 411–421, doi:10.1061/(ASCE)1090-0241(1997)123:5(411).

Minkoff, D. R., M. Escapa, F. E. Ferramola, S. D. Maraschn, J. O. Pierini, G. M. E. Perillo, and C. Delrieux (2006), Effects of crab-halophytic plant interactions on creek growth in a S.W. Atlantic salt marsh: A Cellular Automata model, *Estuarine Coastal Shelf Sci.*, *69*, 403–413, doi:10.1016/j.ecss.2006.05.008.

Möller, I., T. Spencer, J. R. French, D. J. Leggett, and M. Dixon (1999), Wave transformation over salt marshes: A field and numerical modelling study from North Norfolk, England, *Estuarine Coastal Shelf Sci.*, *49*, 411–426, doi:10.1006/ecss.1999.0509.

Morris, J. T. (2006), Competition among marsh macrophystes by means of geomorphological displacement in the intertidal zone, *Estuarine Coastal Shelf Sci.*, *69*, 395–402, doi:10.1016/j.ecss.2006.05.025.

Morris, J. T., and W. B. Bowden (1986), Amechanistic, numerical model of sedimentation, mineralization, and decomposition for marsh sediments, *Soil Sci. Soc. Am. J.*, *50*(1), 96–105.

Morris, J. T., and P. M. Bradley (1999), Effects of nutrient loading on the carbon balance of coastal wetland sediments, *Limnol. Oceanogr.*, *44*(3), 699–702, doi:10.4319/lo.1999.44.3.0699.

Morris, J. T., and B. Haskin (1990), A 5-yr record of aerial primary production and stand characteristics of *Spartina alterniflora*, *Ecology*, *71*(6), 2209–2217, doi:10.2307/1938633.

Morris, J. T., P. V. Sundareshwar, C. T. Nietch, B. Kjerfve, and D. R. Cahoon (2002), Responses of coastal wetlands to rising sea level, *Ecology*, *83*(10), 2869–2877, doi:10.1890/0012-9658(2002)083[2869:ROCWTR]2.0.CO;2.

Morris, J. T., D. Porter, M. Neet, P. A. Noble, L. Schmidt, L. A. Lapine, and J. R. Jensen (2005), Integrating LIDAR elevation data, multi-spectral imagery and neural network modelling for marsh characterization, *Int. J. Remote Sens.*, *26*, 5221–5234, doi:10.1080/01431160500219018.

Mudd, S. M. (2011), The life and death of salt marshes in response to anthropogenic disturbance of sediment supply, *Geology*, *39*(5), 511–512, doi:10.1130/focus052011.1.

Mudd, S. M., S. Fagherazzi, J. T. Morris, and D. J. Furbish (2004), Flow, sedimentation, and biomass production on a vegetated salt marsh in South Carolina: Toward a predictive model of marsh morphologic and ecologic evolution, in *The Ecogeomorphology of Tidal Marshes*, *Coastal and Estuarine Stud.*, vol. 59, edited by S. Fagherazzi, A. Marani, and L. K. Blum, pp. 165–187, AGU, Washington, D. C.

Mudd, S. M., S. M. Howell, and J. T. Morris (2009), Impact of dynamic feedbacks between sedimentation, sea-level rise, and biomass production on near surface marsh stratigraphy and carbon accumulation, *Estuarine Coastal Shelf Sci.*, *82*(3), 377–389, doi:10.1016/j.ecss.2009.01.028.

Mudd, S. M., A. D'Alpaos, and J. T. Morris (2010), How does vegetation affect sedimentation on tidal marshes? Investigating particle capture and hydrodynamic controls on biologically mediated sedimentation, *J. Geophys. Res.*, *115*, F03029, doi:10.1029/2009JF001566.

Nepf, H. M. (1999), Drag, turbulence, and diffusion in flow through emergent vegetation, *Water Resour. Res.*, *35*(2), 479–489, doi:10.1029/1998WR900069.

Neubauer, S. C. (2008), Contributions of mineral and organic components to tidal freshwater marsh accretion, *Estuarine Coastal Shelf Sci.*, *78*(1), 78–88, doi:10.1016/j.ecss.2007.11.011.

Neumeier, U. (2007), Velocity and turbulence variations at the edge of saltmarshes, *Cont. Shelf Res.*, *27*(8), 1046–1059, doi:10.1016/j.csr.2005.07.009.

Neumeier, U., and C. L. Amos (2006), Turbulence reduction by the canopy of coastal *Spartina* salt marshes, *J. Coastal Res.*, *1*, 433–439.

Neumeier, U., and P. Ciavola (2004), Flow resistance and associated sedimentary processes in a *Spartina maritima* salt marsh, *J. Coastal Res.*, *20*, 435–447, doi:10.2112/1551-5036(2004)020[0435:FRAASP]2.0.CO;2.

Novakowski, K. I., R. Torres, L. R. Gardner, and G. Voulgaris (2004), Geomorphic analysis of tidal creek networks, *Water Resour. Res.*, *40*, W05401, doi:10.1029/2003WR002722.

Nyman, J. A., R. J. Walters, R. D. Delaune, and W. H. Patrick (2006), Marsh vertical accretion via vegetative growth, *Estuarine Coastal Shelf Sci.*, *69*(3–4), 370–380, doi:10.1016/j.ecss.2006.05.041.

Ogden, J. C., S. M. Davis, K. J. Jacobs, T. Barnes, and H. E. Fling (2005), The use of conceptual ecological models to guide ecosystem restoration in south Florida, *Wetlands*, *25*(4), 795–809, doi:10.1672/0277-5212(2005)025[0795:TUOCEM]2.0.CO;2.

Orson, R., W. Panageotou, and S. P. Leatherman (1985), Response of tidal salt marshes of the United States Atlantic and Gulf Coasts to rising sea levels, *J. Coastal Res.*, *1*(1), 29–37.

Orton, P. M., and G. C. Kineke (2001), Comparing calculated and observed vertical suspended-sediment distributions from a Hudson River estuary turbidity maximum, *Estuarine Coastal Shelf Sci.*, *52*(3), 401–410, doi:10.1006/ecss.2000.0747.

Palmer, M. R., H. M. Nepf, and T. J. R. Pettersson (2004), Observations of particle capture on a cylindrical collector: Implications for particle accumulation and removal in aquatic systems, *Limnol. Oceanogr.*, *49*(1), 76–85, doi:10.4319/lo.2004.49.1.0076.

Park, R. A., T. V. Armentano, and C. L. Cloonan (1986), Predicting the effects of sea level rise on coastal wetlands, in *Effects of Changes in Stratospheric Ozone and Global Climate*, vol. 4, *Sea Level Rise*, edited by J. G. Titus, pp. 129–152, U.S. Environ. Prot. Agency, Washington, D. C.

Park, R. A., M. S. Trehan, P. W. Mausel, and R. C. Howe (1989), The effects of sea level rise on US coastal wetlands and lowlands, *Coop. Agreement CR814578-01*, final report, U.S. Environ. Prot. Agency, Washington, D. C.

Partheniades, E. (1965), Erosion and deposition of cohesive soils, *J. Hydraul. Div. Am. Soc. Civ. Eng.*, *91*, 105–139.

Perillo, G. M. E., D. Minkoff, and M. Piccolo (2005), Novel mechanism of stream formation in coastal wetlands by crab-fish-groundwater interaction, *Geo-Mar. Lett.*, *25*, 214–220, doi:10.1007/s00367-005-0209-2.

Pestrong, R. (1965), The development of drainage patterns on tidal marshes, *Stanford Publ. Geol. Sci. Tech. Rep. 10*, 87 pp., Stanford Univ., Stanford, Calif.

Pethick, J. S. (1980), Velocity surges and asymmetry in tidal channels, *Estuarine Coastal Mar. Sci.*, *11*, 331–345, doi:10.1016/S0302-3524(80)80087-9.

Pethick, J. S. (1981), Long-term accretion rates on tidal salt marshes, *J. Sediment. Res.*, *51*, 571–577.

Priestas, A. M., and S. Fagherazzi (2011), Morphology and hydrodynamics of wave-cut gullies, *Geomorphology*, *131*(1–2), 1–13, doi:10.1016/j.geomorph.2011.04.004.

Rahmstorf, S. (2007), A semi-empirical approach to projecting future sea-level rise, *Science*, *315*, 368–370, doi:10.1126/science.1135456.

Redfield, A. C. (1965), Ontogeny of a salt marsh estuary, *Science*, *147*, 50–55, doi:10.1126/science.147.3653.50.

Redfield, A. C. (1972), Development of a New England salt marsh, *Ecol. Monogr.*, *42*, 201–237, doi:10.2307/1942263.

Reed, D. J. (1995), The response of coastal marshes to sea-level rise: Survival or submergence?, *Earth Surf Processes Landforms*, *20*, 39–48, doi:10.1002/esp.3290200105.

Reed, D. J., T. Spencer, A. L. Murray, J. R. French, and L. Leonard (1999), Marsh surface sediment deposition and the role of tidal creeks: Implications for created and managed coastal marshes, *J. Coast. Conserv.*, *5*, 81–90, doi:10.1007/BF02802742.

Reyes, E., M. L. White, J. F. Martin, G. P. Kemp, J. W. Day, and V. Aravamuthan (2000), Landscape modeling of coastal habitat change in the Mississippi Delta, *Ecology*, *81*(8), 2331–2349, doi:10.1890/0012-9658(2000)081[2331:LMOCHC]2.0.CO;2.

Reyes, E., et al. (2003), Impacts of sea-level rise on coastal landscapes, in *Preparing for a Changing Climate: The Potential Consequences of Climate Variability and Change—Gulf Coast Region.*, edited by Z. H. Ning et al., pp. 105–114, Gulf Coast Clim. Change Assess. Counc. and La. St. Univ. Graphic Serv., Baton Rouge, La.

Reyes, E., et al. (2004a), Assessing coastal management plans using watershed spatial models for the Mississippi Delta, USA, and the Usumacinta-Grijalva Delta, Mexico, *Ocean Coast. Manage.*, *47*, 693–708, doi:10.1016/j.ocecoaman.2004.12.008.

Reyes, E., et al. (2004b), River forcing at work: Ecological modeling of prograding and regressive deltas, *Wetlands Ecol. Manage.*, *12*, 103–114, doi:10.1023/B:WETL.0000021663.50750.45.

Rinaldo, A., S. Fagherazzi, S. Lanzoni, M. Marani, and W. E. Dietrich (1999a), Tidal networks: 2. Watershed delineation and comparative network morphology, *Water Resour. Res.*, *35*(12), 3905–3917, doi:10.1029/1999WR900237.

Rinaldo, A., S. Fagherazzi, S. Lanzoni, M. Marani, and W. E. Dietrich (1999b), Tidal networks: 3. Landscape-forming discharges and studies in empirical geomorphic relationships, *Water Resour. Res.*, *35*(12), 3919–3929, doi:10.1029/1999WR900238.

Rodriguez-Iturbe, I., and A. Rinaldo (1997), *Fractal River Basins: Chance and Self-Organization*, Cambridge Univ. Press, New York.

Rybczyk, J. M., and D. R. Cahoon (2002), Estimating the potential for submergence for two wetlands in the Mississippi River Delta, *Estuaries*, *25*(5), 985–998, doi:10.1007/BF02691346.

Rybczyk, J. M., and J. C. Callaway (2009), Surface elevation models, in *Coastal Wetlands: An Ecosystem Integrated Approach*, edited by G. M. E. Perillo et al., pp. 834–853, Elsevier, Amsterdam.

Rybczyk, J. M., J. C. Callaway, and J. W. Day (1998), A relative elevation model for a subsiding coastal forested wetland receiving wastewater effluent, *Ecol. Modell.*, *112*(1), 23–44, doi:10.1016/S0304-3800(98)00125-2.

Sharma, P., L. R. Gardner, W. S. Moore, and M. S. Bollinger (1987), Sedimentation and bioturbation in a salt marsh as revealed by Pb-210, Cs-137, and Be-7 studies, *Limnol. Oceanogr.*, *32*(2), 313–326, doi:10.4319/lo.1987.32.2.0313.

Silver, W. L., and R. K. Miya (2001), Global patterns in root decomposition: Comparisons of climate and litter quality effects, *Oecologia*, *129*(3), 407–419.

Silvestri, S., A. Defina, and M. Marani (2005), Tidal regime, salinity and salt marsh plant zonation, *Estuarine Coastal Shelf Sci.*, *62*(1–2), 119–130, doi:10.1016/j.ecss.2004.08.010.

Sklar, F. H., et al. (1985), Dynamic spatial simulation modelling of coastal wetland habitat succession, *Ecol. Modell.*, *29*, 261–281, doi:10.1016/0304-3800(85)90056-0.

Sklar, F. H., et al. (1990), Model conceptualization, in *Wetlands and Shallow Continental Water Bodies*, vol. 1, edited by B. C. Patten, chap. 27, pp. 625–658, SPB Acad. Publ., Amsterdam.

Solari, L., G. Seminara, S. Lanzoni, M. Marani, and A. Rinaldo (2002), Sand bars in tidal channels: Part 2. Tidal meanders, *J. Fluid Mech.*, *451*, 203–238, doi:10.1017/S0022112001006565.

Soulsby, R. L. and Dyer, K. R. (1981) The form of the near-bed velocity profile in a tidally accelerating flow, *J. Geophys. Res.*, *86*(C9), 8067–8074, doi:10.1029/JC086iC09p08067.

Spalding, E. A., and M. W. Hester (2007), Interactive effects of hydrology and salinity on oligohaline plant species productivity: Implications of relative sea-level rise, *Estuaries Coasts*, *30*(2), 214–225.

Stapleton, K. R., and D. A. Huntley (1995), Seabed stress determinations using the inertial dissipation method and the turbulent kinetic energy method, *Earth Surface Processes Landforms*, *20*(9), 807–815.

Steel, T. J., and K. Pye (1997) The development of saltmarsh tidal creek networks: Evidence from the UK, in *Proceedings of the Canadian Coastal Conference, University of Guelph, 22–25 May 1997*, pp. 267–280, Can. Coastal Sci. and Eng. Assoc., Burlington, Ont., Canada.

Steers, J. A. (1960), Physiography and evolution: The physiography and evolution of Scolt Head Island, in *Scolt Head Island*, 2nd ed., edited by J. A. Steers, pp. 12–66, Heffer, Cambridge, U. K.

Stefanon, L., L. Carniello, A. D'Alpaos, and S. Lanzoni (2010), Experimental analysis of tidal network growth and development, *Cont. Shelf Res.*, doi:10.1016/j.csr.2009.08.018.

Stevenson, J. C., L. G. Ward, and M. S. Kearney (1986), Vertical accretion in marshes with varying rates of sea-level rise, in *Estuarine Variability*, edited by D. A. Wolfe, pp. 241–259, Academic, Orlando, Fla.

Stoddart, D. R., D. J. Reed, and J. R. French (1989), Understanding salt marsh accretion, Scolt Head Island, Norfolk, England, *Estuaries*, *12*(4), 228–236, doi:10.2307/1351902.

Struyf, E., S. Temmerman, and P. Meire (2007), Dynamics of biogenic Si in freshwater tidal marshes: Si regeneration and retention in marsh sediments (Scheldt Estuary), *Biogeochemistry*, *82*, 41–53, doi:10.1007/s10533-006-9051-5.

Stumpf, R. P. (1983), The process of sedimentation on the surface of a salt marsh, *Estuarine Coastal Shelf Sci.*, *17*, 495–508, doi:10.1016/0272-7714(83)90002-1.

Swenson, E. M., and C. M. Swarzenski (1995), Water levels and salinity in the Barataria –Terrebonne estuarine system, in *Status and Historical Trends of Hydrologic Modification, Reduction in Sediment Availability, and Habitat Loss/Modification in the Barataria and Terrebonne Estuarine Systems. BTNEP Publ. 20*, edited by D. J. Reed, pp. 129–201, Barataria-Terrebonne Natl. Estuary Program, Thibodaux, La.

Tanino, Y., and H. M. Nepf (2008), Laboratory investigation of mean drag in a random array of rigid, emergent cylinders, *J. Hydraul. Eng.*, *134*(1), 34–41, doi:10.1061/(ASCE)0733-9429(2008)134:1(34).

Temmerman, S., G. Govers, P. Meire, and S. Wartel (2003a), Modelling long-term tidal marsh growth under changing tidal conditions and suspended sediment concentrations, Scheldt Estuary, Belgium, *Mar. Geol.*, *193*, 151–169, doi:10.1016/S0025-3227(02)00642-4.

Temmerman, S., G. Goers, S. Wartel, and P. Meire (2003b), Spatial and temporal factors controlling short-term sedimentation in a salt and freshwater tidal marsh, Scheldt Estuary, Belgium, SW Netherlands, *Earth Surf Processes Landforms*, *28*, 739–755, doi:10.1002/esp.495.

Temmerman, S., G. Govers, P. Meire, and S. Wartel (2004), Simulating the long-term development of levee-basin topography on tidal marshes, *Geomorphology*, *63*(1–2), 39–55, doi:10.1016/j.geomorph.2004.03.004.

Temmerman, S., T. J. Bouma, G. Govers, and D. Lauwaet (2005a), Flow paths of water and sediment in a tidal marsh: Relations with marsh developmental stage and tidal inundation height, *Estuaries*, *28*(3), 338–352, doi:10.1007/BF02693917.

Temmerman, S., T. J. Bouma, G. Govers, Z. B. Wang, M. B. De Vries, and P. M. J. Herman (2005b), Impact of vegetation on flow routing and sedimentation patterns: Three-dimensional modeling for a tidal marsh, *J. Geophys. Res.*, *110*, F04019, doi:10.1029/2005JF000301.

Temmerman, S., T. J. Bouma, J. Van de Koppel, D. Van der Wal, M. B. De Vries, and P. M. J. Herman (2007), Vegetation causes channel erosion in a tidal landscape, *Geology*, *35*(7), 631–634, doi:10.1130/G23502A.1.

Tonelli, M., S. Fagherazzi, and M. Petti (2010), Modeling wave impact on salt marsh boundaries, *J. Geophys. Res.*, *115*, C09028, doi:10.1029/2009JC006026.

Torres, R., and R. Styles (2007), Effects of topographic structure on salt marsh currents, *J. Geophys. Res.*, *112*, F02023, doi:10.1029/2006JF000508.

Townend, I. H., C. A. Fletcher, M. A. F. Knaapen, and S. K. Rossington (2010), A review of salt marsh dynamics, *Water Environ. J.*, *24*, 1–12.

Turner, R. E., E. M. Swenson, and C. S. Milan (2001), Organic and inorganic contributions to vertical accretion in salt marsh sediments, in *Concepts and Controversies in Tidal Marsh Ecology*, edited by M. Weinstein and K. Kreeger, pp. 583–595, Kluwer Acad., Dordrecht, Netherlands.

Van de Koppel, J., D. Van der Wal, J. P. Bakker, and P. M. J. Herman (2005), Self-organization and vegetation collapse in salt marsh ecosystems, *Am. Nat.*, *165*, E1–E12, doi:10.1086/426602.

van de Plassche, O., K. van der Borg, and A. F. M. de Jong (1998), Sea level–climate correlation during the past 1400 yr, *Geology*, *26*, 319–322.

van der Wal, D., and K. Pye (2004), Patterns, rates, and possible causes of salt marsh erosion in the Greater Thames area (UK), *Geomorphology*, *61*(3–4), 373–391, doi:10.1016/j.geomorph.2004.02.005.

van der Wal, D., A. Wielemaker-Van den Dool, and P. M. J. Herman (2008), Spatial patterns, rates and mechanisms of saltmarsh cycles (Westerschelde, the Netherlands), *Estuarine Coastal Shelf Sci.*, *76*, 357–368, doi:10.1016/j.ecss.2007.07.017.

Van Proosdij, D., R. G. D. Davidson-Arnott, and J. Ollerhead (2006), Controls on spatial patterns of sediment deposition across a macro-tidal salt marsh surface over single tidal cycles, *Estuarine Coastal Shelf Sci.*, *69*, 64–86, doi:10.1016/j.ecss.2006.04.022.

Wallace, K. J., J. C. Callaway, and J. B. Zedler (2005), Evolution of tidal creek networks in a high sedimentation environment: A 5-year experiment at Tijuana Estuary, California, *Estuaries*, *28*(6), 795–811, doi:10.1007/BF02696010.

Wang, F. C., et al. (1993), Intertidal marsh suspended sediment transport processes, Terrebonne Bay, Louisiana, USA, *J. Coastal Res.*, *9*(1), 209–220.

Weinstein, M. P., and D. A. Kreeger (2000), *Concepts and Controversies in Tidal Marsh Ecology*, 864 pp., Springer, New York.

Woolnough, S. J., J. R. L. Allen, and W. L. Wood (1995), An exploratory numerical model of sediment deposition over tidal marshes, *Estuarine Coastal Shelf Sci.*, *41*, 515–543, doi:10.1016/0272-7714(95)90025-X.

Yang, S. L. (1998), The role of Scirpus marsh in attenuation of hydrodynamics and retention of fine sediment in the Yangtze Estuary, *Estuarine Coastal Shelf Sci.*, *47*, 227–233, doi:10.1006/ecss.1998.0348.

Yang, S. L., H. Li, T. Ysebaert, T. J. Bouma, W. X. Zhang, Y. Wang, P. Li, M. Li, and P. Ding (2008), Spatial and temporal variations in sediment grain size in tidal wetlands, Yangtze Delta: On the role of physical and biotic controls, *Estuarine Coastal Shelf Sci.*, *77*(4), 657–671, doi:10.1016/j.ecss.2007.10.024.

Yapp, R. H., D. Johns, and O. T. Jones (1916), The salt marshes of the Dovey Estuary: Part I. Introductory, *J. Ecol.*, *4*, 27–42, doi:10.2307/2255448.

Yapp, R. H., D. Johns, and O. T. Jones (1917) The salt marshes of the Dovey Estuary: Part II. The salt marshes, *J. Ecol.*, *5*, 65–103.

J. Clough, Warren Pinnacle Consulting, PO Box 253, Warren, VT 05674, USA.

C. Craft, School of Public and Environmental Affairs, Indiana University, MSB II Rm. 408, 702 N. Walnut Grove Ave., Bloomington, IN 47405, USA.

A. D'Alpaos, Department of Geosciences, University of Padova, via Gradenigo 6, Padova PD I-35131, Italy.

S. Fagherazzi, Department of Earth Sciences, Boston University, 675 Commonwealth Ave., Boston, MA 02215, USA. (sergio@bu.edu)

G. R. Guntenspergen, Patuxent Wildlife Research Center, U.S. Geological Survey, 12100 Beech Forest Rd., Ste. 4039, Laurel, MD 20708–4039, USA.

M. L. Kirwan, Department of Environmental Sciences, University of Virginia, PO Box 400123, Charlottesville, VA 22904, USA.

S. M. Mudd, Institute of Geography, School of GeoSciences, University of Edinburgh, Drummond Street, Edinburgh EH8 9XP, UK.

E. Reyes, Department of Biology, East Carolina University, N108 Howell Science Complex, Greenville, NC 27858–4353, USA.

J. M. Rybczyk, Department of Environmental Sciences, Huxley College of the Environment, Western Washington University, 516 High St., MS 9181, Bellingham, WA 98225, USA.

S. Temmerman, Department of Biology, University of Antwerpen, Universiteitsplein 1, Antwerpen B-2610, Belgium.

J. van de Koppel, Spatial Ecology Department, NIOO-KNAW, Korringaweg 7, Yerseke NL-4401 NT, Netherlands.